

Hydrogen and Fuel Cells Program
2019 Annual Merit Review and Peer Evaluation Meeting
Arlington, VA – April 29 - May 1, 2019



ElectroCat (Electrocatalysis Consortium)

Piotr Zelenay

Los Alamos National Laboratory
Los Alamos, New Mexico 87545

Deborah Myers

Argonne National Laboratory
Lemont, Illinois 60439



Project ID: FC160

Timeline

- Start date (launch): Feb 1, 2016
- End date: Sep 30, 2020

Budget

- FY18 funding total: \$4,021k
- FY19 core funding: \$3,900k
- FY17 FOA projects support: \$746k
- FY19 funding total: \$4,646k

Barriers

- A. Cost (catalyst)
- D. Activity (catalyst; MEA)
- B. Durability (catalyst; MEA)
- C. Power density (MEA)

Partner

– PI

Los Alamos National Laboratory



– Piotr Zelenay

Argonne National Laboratory



– Deborah Myers

National Renewable Energy Laboratory



– K. C. Neyerlin

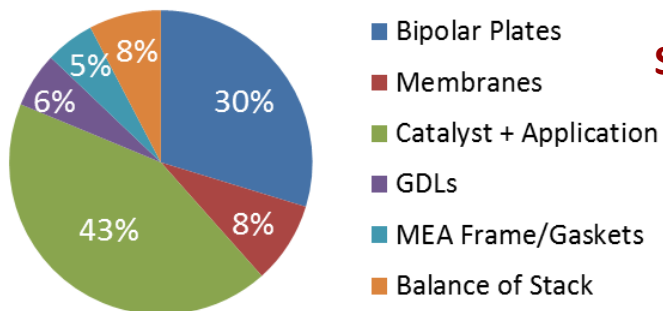
Oak Ridge National Laboratory



– Karren More

Relevance: Fuel Cell Stack Cost Challenge

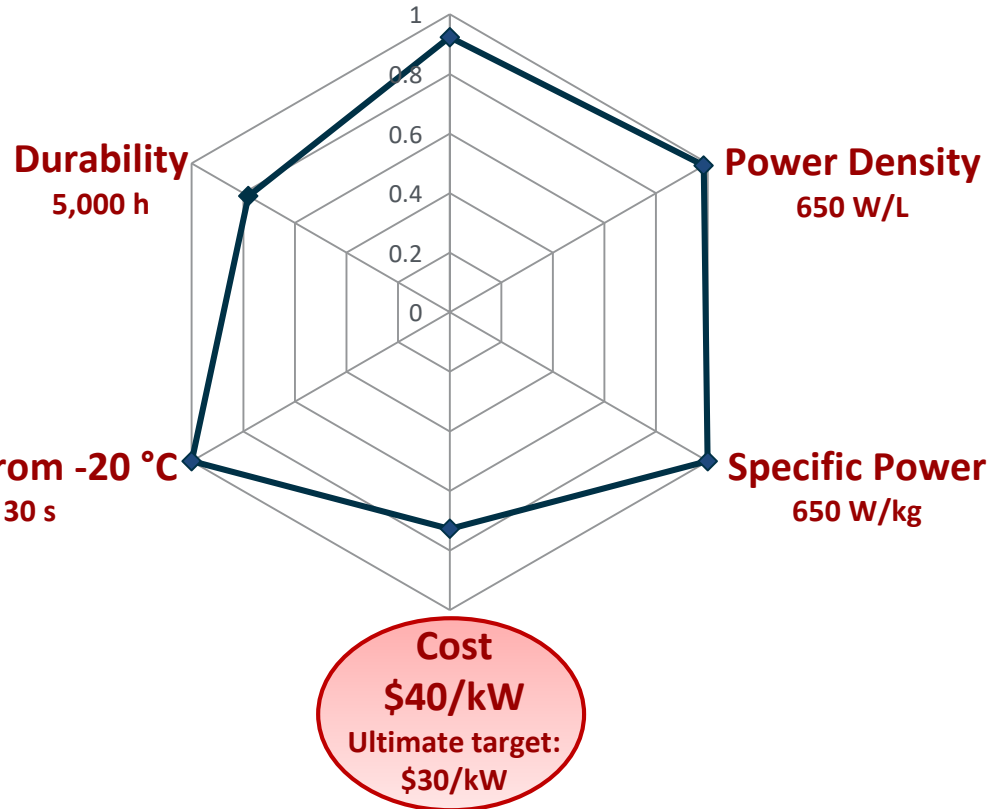
PGM Stack Cost Breakdown (500,000 systems/year)



https://www.hydrogen.energy.gov/pdfs/16020_fuel_cell_system_cost_2016.pdf

PGM-based System Automotive Stack Status

Peak Energy Efficiency



ElectroCat created as part of



Energy Materials Network in February 2016
U.S. Department of Energy

Goal: Accelerate the deployment of fuel cell systems by eliminating the use of PGM catalysts

Approach: ElectroCat Objectives and Lab Roles

Mission: Develop and implement PGM-free catalysts and electrodes by streamlining access to unique synthesis and characterization tools across national labs, developing missing strategic capabilities, and curating a public database of information.

Materials Discovery and Development	Catalysts for oxygen reduction in low-temperature PEFCs and PAFCs
	Catalysts for oxygen reduction and hydrogen oxidation in AMFCs
	Development of electrodes and MEAs compatible with PGM-free catalysts
Tool Development	Optimization of atomic-scale and mesoscale models of catalyst activity to predict macro-scale behavior
	High-throughput techniques for catalyst synthesis
	High-throughput techniques for characterization of catalysts, electrodes, and MEAs
	Aggregation of data in an easily searchable, public database to facilitate the development of catalyst materials and MEAs



LANL: PGM-free catalyst development, electrochemical and fuel cell testing, atomic-scale modeling

ANL: High-throughput techniques, mesoscale models, X-ray studies, aqueous stability studies

NREL: Advanced fuel cell characterization, high-throughput electrode fabrication and testing

ORNL: Advanced electron microscopy, atomic-level characterization, XPS studies

Approach: FY18 ElectroCat Milestone; FY19 LANL QPMs

FY18

September 2018 (FY18 Q4)	Achieve PGM-free cathode MEA performance in an H ₂ -O ₂ fuel cell of 25 mA cm ⁻² at 0.90 V (<i>iR</i> -corrected) at 1.0 bar partial pressure of O ₂ and cell temperature 80°C; define performance-limiting catalyst and electrode properties to guide the synthesis of PGM-free catalysts and fabrication of electrodes/MEAs (LANL, ANL, ORNL, NREL).	Completed High of 36 mA cm ⁻² , average of 33 mA cm ⁻² reached at 0.90 V (see slide 11 for details)

FY19

December 2018 (FY19 Q1)	Propose modifications to the electrode structure to improve mass transport in the high current density region based on studies of ionomer loading gradient and improved porosity using CL pore formers.	Completed (see slide 30)
March 2019 (FY19 Q2)	Identify the relation between MOF synthesis conditions and ORR activity through a systematic study and propose a possible synthesis pathway(s) to improve the catalyst ORR activity and durability. Demonstrate the MEA durability decay rate of $\leq 1 \text{ mA}/(\text{cm}^2 \text{ h})$ at 0.7 V at 0.2 bar partial pressure of O ₂ and cell temperature 80 °C.	On track
March 2019 (FY19 Q2)	Demonstrate the ability of <i>Adaptive Design</i> to utilize input data from ANL curated data format and output DFT data to ANL curated data format. This will enable concurrent evolution of the experimental and theoretical databases with all appropriate metadata.	On track
June 2019 (FY19 Q3)	Complete of X-ray and vibrational spectra calculations for FeN ₄ , OHFeN ₄ , and OFeN ₄ hosted at zig-zag edge, arm-chair edge and in the bulk, as well as N- and C-degraded OHFeN ₄ active sites structures with and without NO probe molecule. Compare calculation results to experimental signatures (XANES, NRVS, EELS, etc.).	On track
September 2019 (FY19 Q4)	Identify mechanisms of Fe de-metalation based on the systematic analysis proposed in Task 6. Provide a complete analysis of the kinetic degradation model at varied voltage, partial pressures, and relative humidity conditions. Demonstrate improved durability of PGM-free electrocatalysts during fuel cell operation based on mitigation mechanisms developed from the knowledge gained from the mitigation of catalyst degradation task.	On track

Approach: FY19 LANL & ANL Capability Go/No-Go Decisions; ANL QPMs

Date	LANL Capability Go/No-Go	Status
September 2019 (FY19 Q4)	Provide demonstration report on model developments with prediction of further optimized synthesis pathway based on high-throughput synthesis data.	On track

Date	ANL Quarterly Progress Measures	Status
December 2018 (FY19 Q1)	Synthesize 25 unique Fe,TM-N-C catalysts using high-throughput methodology and evaluate their ORR activity and activity durability using hydrodynamic, high-throughput techniques. Goal for area-specific ORR activity of 70 $\mu\text{A}/\text{mF}$ at 0.8 V.	Completed (see slides 23 and 24)
March 2019 (FY19 Q2)	Fully define the structure of PGM-free electrodes and agglomerates by supplementing nano-CT data with information from other techniques, such as small angle X-ray scattering, porosimetry, TEM, etc.	On track
June 2019 (FY19 Q3)	Determine the sources of high current density performance limitations for PGM-free electrodes.	On track
June 2019 (FY19 Q3)	(1) Publish database of DFT calculations and the raw input and output files; (2) make openly available the curated data gathered in HT synthesis and characterization effort; (3) create and ingest containerized models into DLHub with links to data in MDF to promote reuse and replicability.	On track
September 2019 (FY19 Q3)	Define catalyst composition, synthetic procedure, and electrode composition that will achieve a 20% improvement in cathode performance lifetime versus the 2018 ElectroCat status (duration over which current density at 0.7 V with hydrogen-air shows < 5% decay).	On track

Date	ANL Capability Go/No-Go	Status
March 2019 (FY19 Q2)	Quantify the amount and relative adsorption energies (i.e., desorption temperatures) of NO adsorbed on different surface sites on the (AD)Fe N C catalyst. Correlate the site density with the stripping charges determined using cyclic voltammetry.	On track
September 2019 (FY19 Q4)	Provide demonstration report on model developments with prediction of further optimized synthesis pathway based on high-throughput synthesis data.	On track

Approach: FY19 ORNL & NREL QPMs

December 2018 (FY19 Q1)	Initiate STEM imaging and spectroscopy for at least three (3) electrospun PGM-free catalysts, before and after incorporation into an MEA. Progress measure will be coordinated with NREL to assess structure and uniformity of catalyst layers fabricated and to correlate morphological observations with measured performance.	Completed
March 2019 (FY19 Q2)	Characterize at least three (3) MOF-based PGM-free catalysts incorporated in the cathode catalyst layer of MEAs before and after durability testing using high-resolution analytical electron microscopy. Coordinate analysis effort and MEAs with tasks for implementing PGM-free catalyst test protocols at LANL and tasks for X-ray scattering and nano-CT at ANL .	On track
June 2019 (FY19 Q3)	Report on effort to measure Fe demetalation in several PGM-free MEAs after fuel cell operation/testing using STEM/EELS/EDS and XPS. Effort will be highly coordinated with LANL and ANL to quantify the loss of Fe relating directly to loss of Fe-based catalytic sites in PANI- and MOF-derived catalysts.	On track

December 2018 (FY19 Q1)	Completion of an X-Ray Diffraction Analysis tool, to be integrated into the Data Hub and available as an analysis tool for XRD result data. We will work with ElectroCat researchers to confirm applicability of the tool on at least 2 XRD datasets in the ElectroCat Data Hub.	Completed
March 2019 (FY19 Q2)	Characterize bulk electrode transport resistance as a function of electrode fabrication conditions. Improve bulk electrode transport resistance by at least 10% when compared to ultrasonically sprayed CCMs deposited at 80 °C (our current standard).	Completed
June 2019 (FY19 Q3)	Elucidate trends in drying rate on in-situ MEA performance and durability utilizing the segmented cell. Down-selected high-performing regimes will be assessed for transport and proton resistance.	On track
August 2019 (FY19 Q4)	In accordance with the annual ElectroCat milestone in Q4 of FY19, demonstrate the ability to reduce bulk electrode transport resistance by 10% over ultrasonically sprayed electrodes, when utilizing ink and/or processing methodologies.	On track

Approach: FY19 NREL Go/No-Go Decisions; FY19 ElectroCat Milestone

Date	NREL Capability Go/No-Go	Status
June 2019 (FY19 Q3)	For an identical catalyst material, loading and operating condition, demonstrate that electrospun fabricated electrodes exhibit a 10% improvement in performance as determined at constant potential (between 0.6 and 0.4 V), when compared to electrodes fabricated via ultrasonic spray or hand-painting.	On track
August 2019 (FY19 Q4)	Compute onset potentials for ORR on FeN_4 structure (with and without OH ligands) on graphene. Calculate a potential value for where the OH occupied site is favored vs. the computational hydrogen electrode (CHE) prediction. Determine the source of deviations, and analyze the effect of different contributions, e.g. entropic effects, solvent effects, etc. If differences in the potential value are obtained vs the CHE and the differences due to different contributions can be understood, then the capability is a Go.	On track

Date	ElectroCat Annual Milestone	Status
September 2019 (FY19 Q4)	Achieve PGM-free cathode MEA performance in an $\text{H}_2\text{-O}_2$ fuel cell of 29 mA cm^{-2} at 0.90 V (iR -corrected) at 1.0 bar partial pressure of O_2 and cell temperature 80°C ; define performance-limiting catalyst and electrode properties to guide the synthesis of PGM-free catalysts and fabrication of electrodes/MEAs (LANL, ANL, ORNL, NREL).	First part completed; second part on track

Collaboration and Coordination: Summary

ElectroCat members: Four national laboratories:



Los Alamos National Laboratory – ElectroCat co-Lead

Argonne National Laboratory – ElectroCat co-Lead

National Renewable Energy Laboratory

Oak Ridge National Laboratory

Support of ten FY2017 FOA, FY2019 FOA, FY2019 Lab Call projects (see next slide for lead organizations)

Collaborators not directly participating in ElectroCat (no-cost):



CRESCENDO, European fuel cell consortium focusing on PGM-free electrocatalysis – development and validation of PGM-free catalyst test protocols



PEGASUS, European fuel cell consortium targeting PGM-free fuel cells – development and validation of PGM-free catalyst test protocols



Israeli Fuel Cell Consortium (IFCC) – PGM-free activity indicators and durability



Bar-Ilan University, Israel – aerogels-based catalysts with high active-site density



University at Buffalo (SUNY), Buffalo, New York – novel PGM-free catalyst synthesis (independent of two ElectroCat projects involving UB)



Pajarito Powder, Albuquerque, New Mexico – catalyst scale-up, PGM-free electrode design, catalyst commercialization



Technical University Darmstadt, Germany – catalyst characterization by Mössbauer spectroscopy and synchrotron X-ray techniques



University of Warsaw, Poland – role of graphite in PGM-free catalyst design



Chevron Energy Technology Company, Richmond, California – patent application with LANL on non-electrochemical uses of PGM-free carbon-based materials

Collaboration & Coordination: Current ElectroCat Projects

Core: FY2016



FY2017 FOA



FY2019 FOA



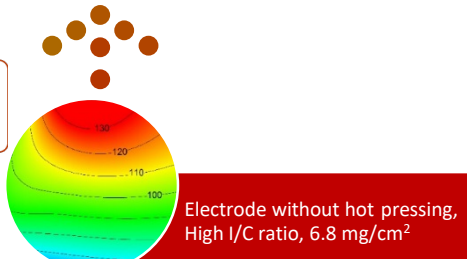
ElectroCat FY18 Annual Milestone Exceeded

Anode: 0.2 mg_{Pt} cm⁻² Pt/C H₂, 200 sccm, 1.0 bar H₂ partial pressure; **Cathode:** ca. 6.8 mg cm⁻², CM-PANI-Fe-C(Zn), Aquion[®] D83 55 wt%, 200 sccm, 1.0 bar O₂ partial pressure; **Membrane:** Nafion[®] 211; **Cell:** 5 cm²

FY18 Milestone: 25 mA/cm² at 0.90 V (iR-free)

Voltage hold at 0.3 V in H₂-air/O₂ while heated up to 80°C

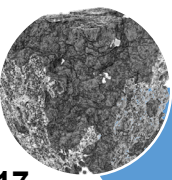
Conditioned in humidified N₂ at 80°C, short break-in at 0.8 V in H₂-O₂



Prior to 2018

2018

2017



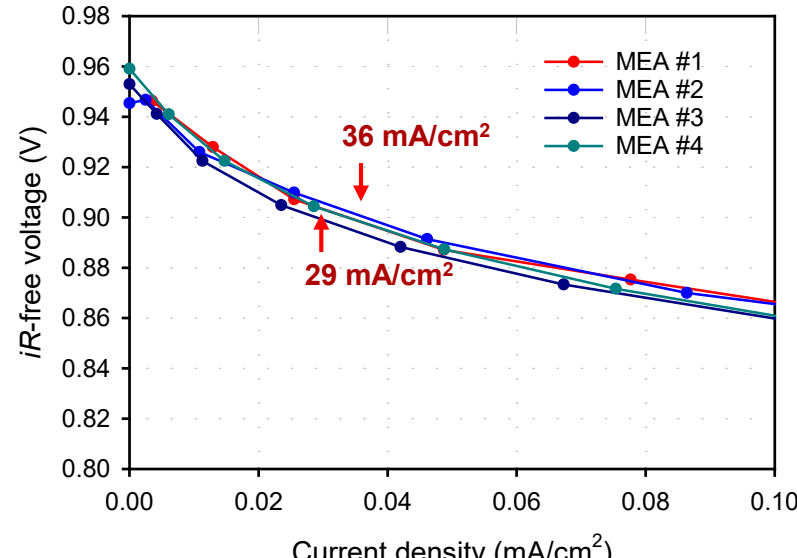
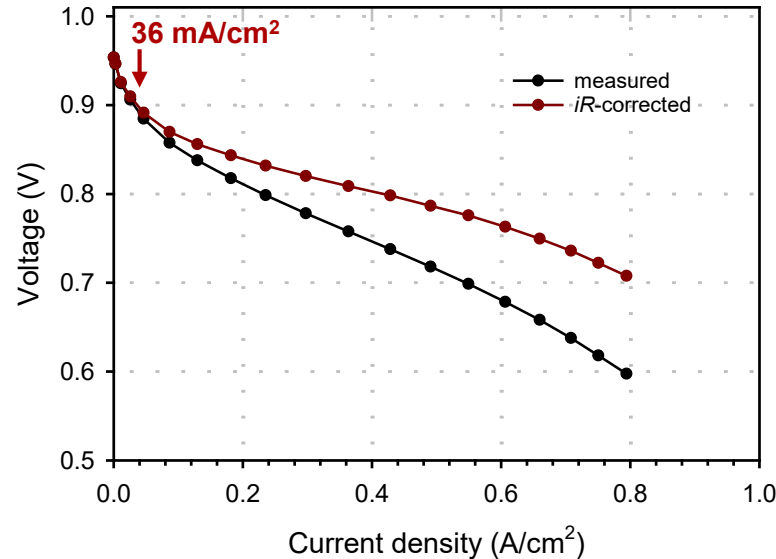
Hot pressed electrode
Low I/C ratio, 3.5 mg/cm²

Electrode without hot pressing,
Optimized I/C ratio, 4.5 mg/cm²

Prior to 2017

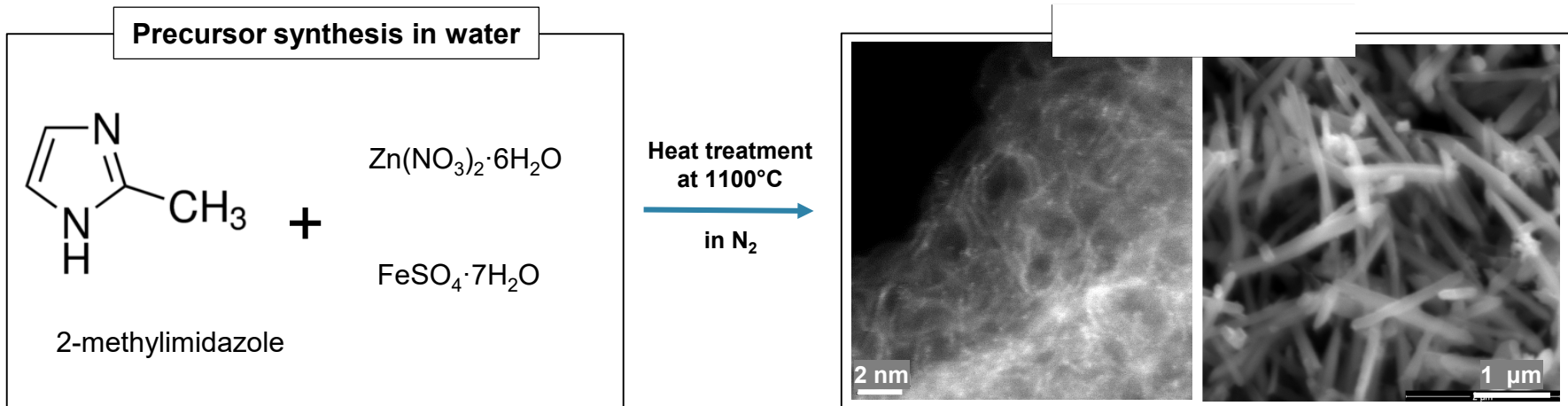
Current density of **36 mA cm⁻²** (mean of 33 mA cm⁻²) at 0.90 V (iR-free) reached in H₂-O₂ fuel cell with CM-PANI-Fe-C(Zn) catalyst

ElectroCat FY18 Annual Milestone of 25 mA cm⁻² at 0.90 V achieved and exceeded!

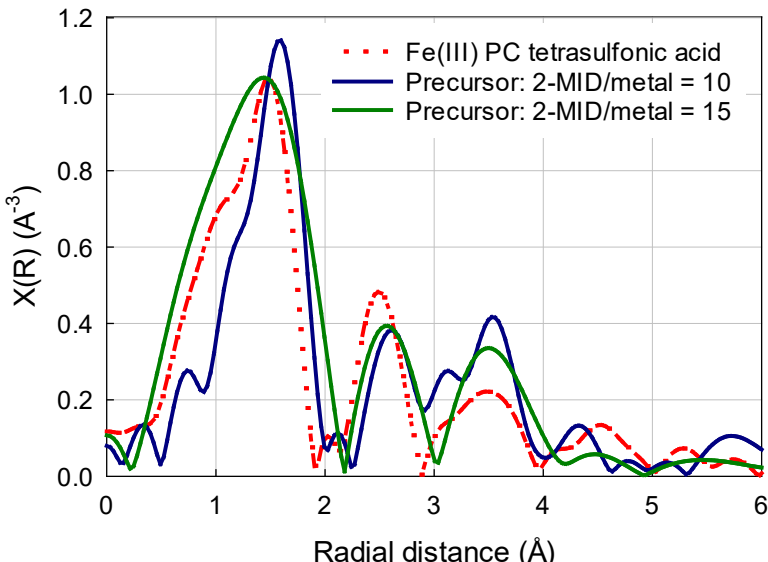


(AD)Fe-N-C Catalyst: Maximizing FeN_4 Content in Precursor

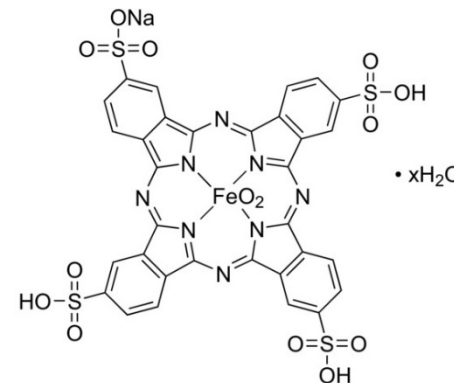
Simple synthesis of (AD)Fe-N-C catalysts through dual metal (Zn, Fe)-ZIFs



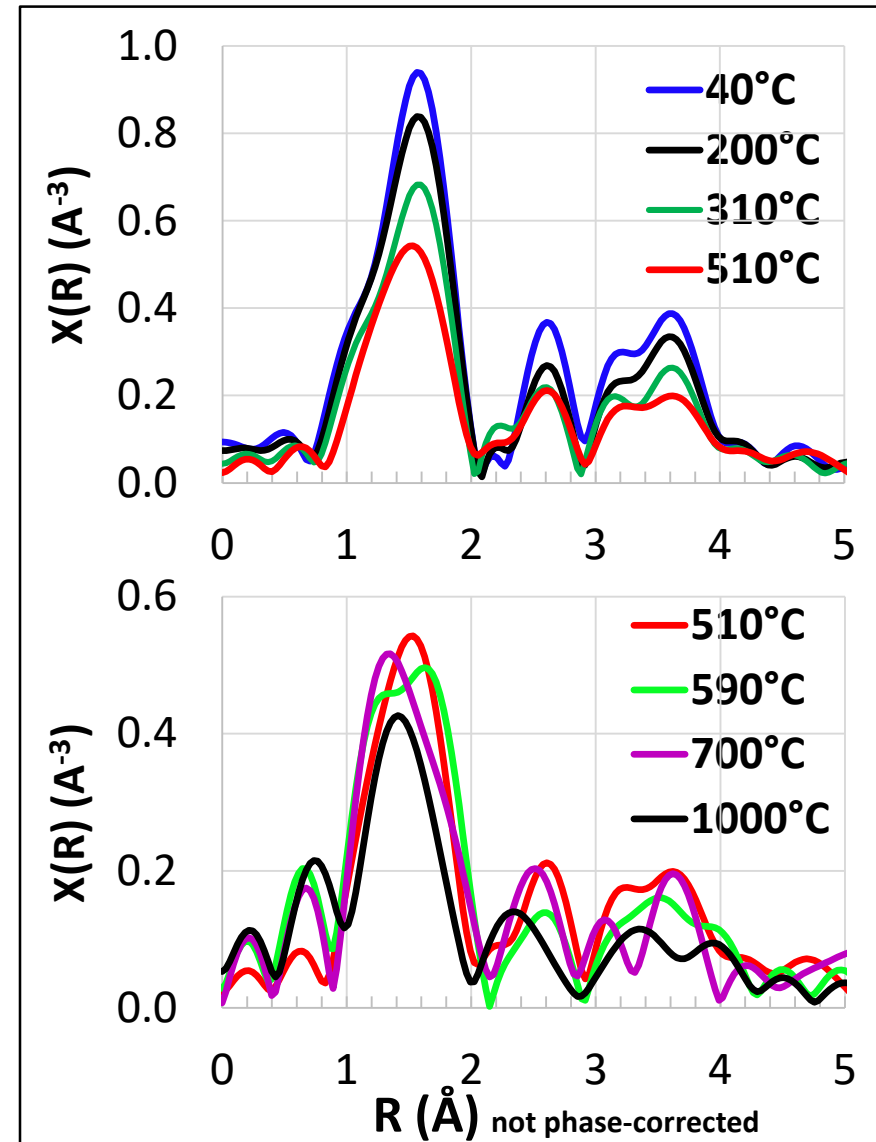
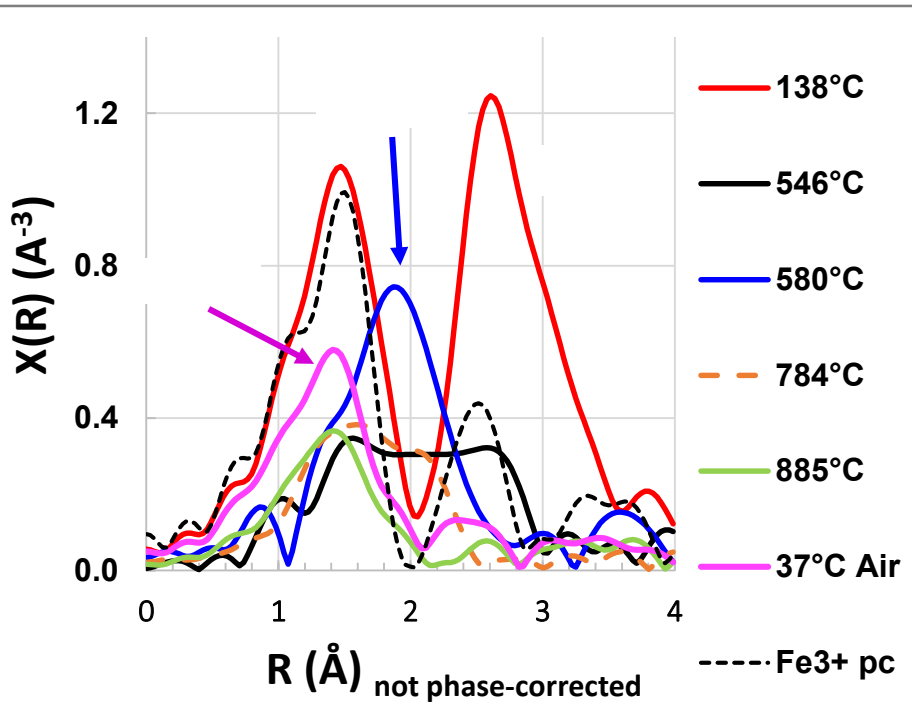
FeN₄ moiety in ZIF precursor confirmed by EXAFS



[reference: Fe(III) PC tetrasulfonic acid]

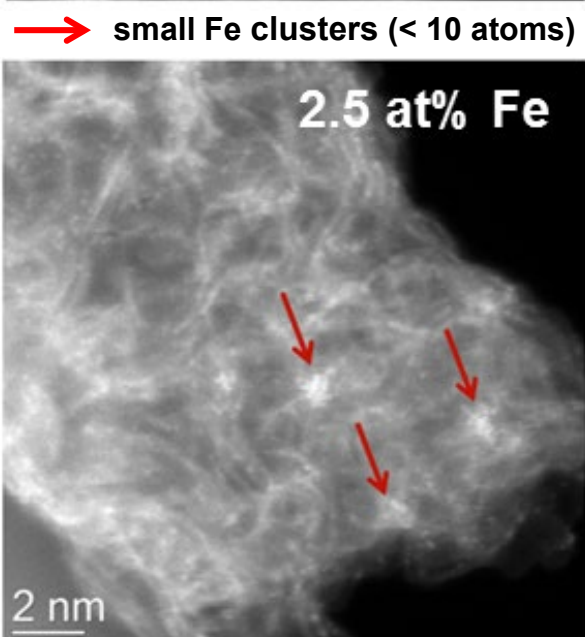
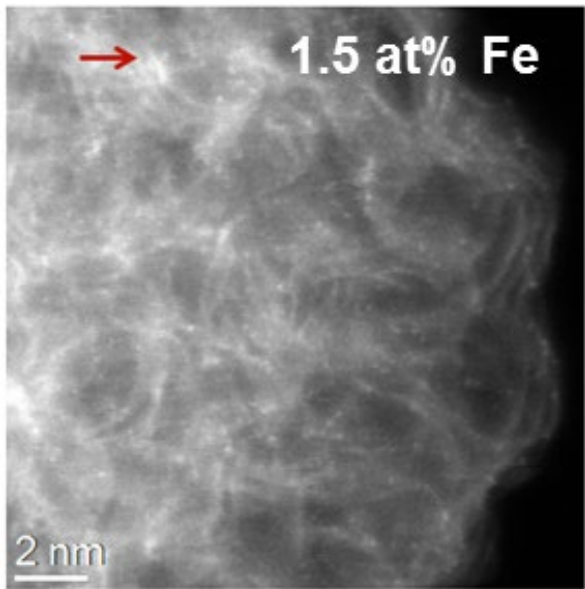


Fe Coordination in Fe_xZn_y ZIF During Heat Treatment

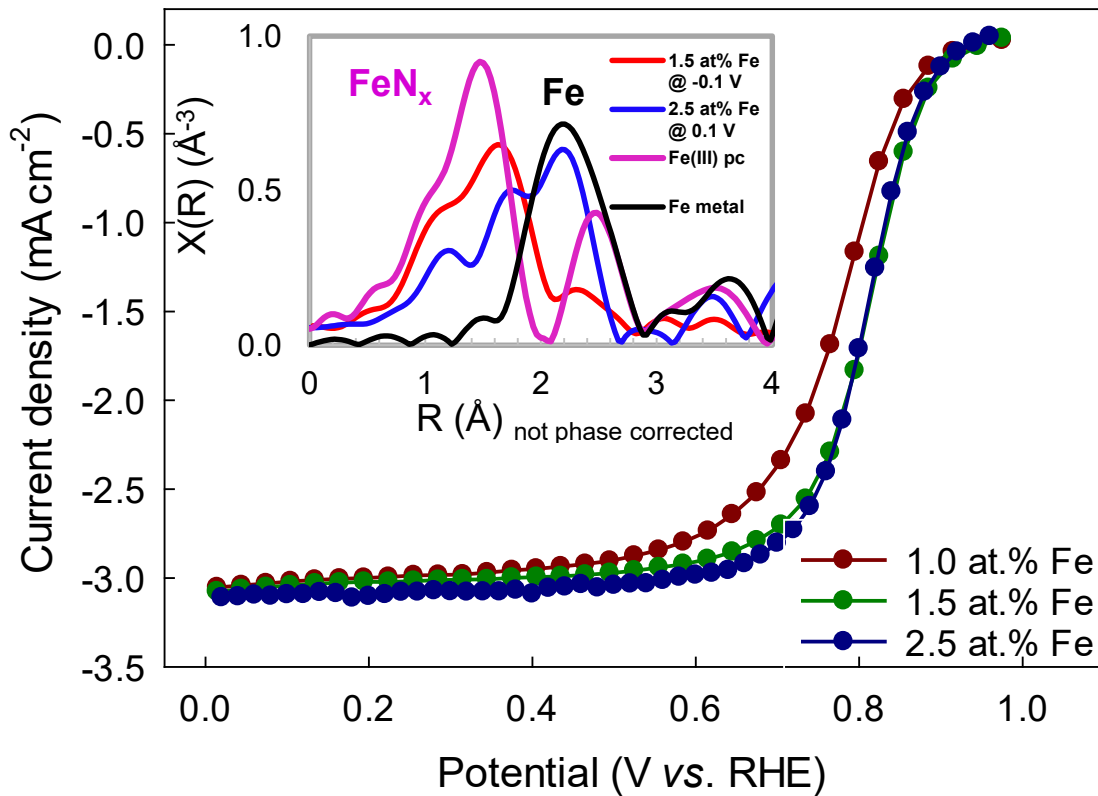


- $\text{Fe}_{2.5}\text{Zn}_{97.5}$ ZIF exhibiting Fe_2O_3 -like coordination and transitioning through Fe carbide to FeN_x
 - ✓ Fe-N 3.9 ± 0.5 before air exposure
 - ✓ Fe-N,O 4.5 ± 0.5 after air exposure
- $\text{Fe}_{1.5}\text{Zn}_{98.5}$ ZIF in FeN_x -like coordination, transitioning through FeN_x species with shorter bond length

(AD)Fe-N-C Catalyst: Dependence of ORR Activity on Fe Content

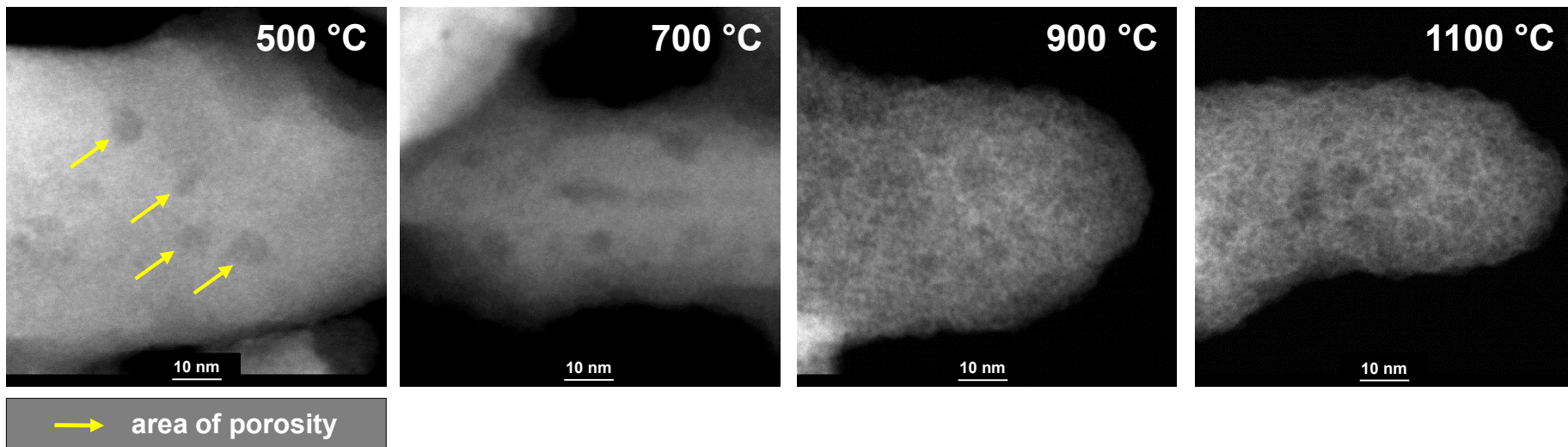


ORR: 0.6 mg cm⁻²; 0.5 M H₂SO₄; 900 rpm; 25°C; Ag/AgCl (saturated KCl) reference electrode; graphite counter electrode; steady-state potential program: 20 mV steps, 20 s/step

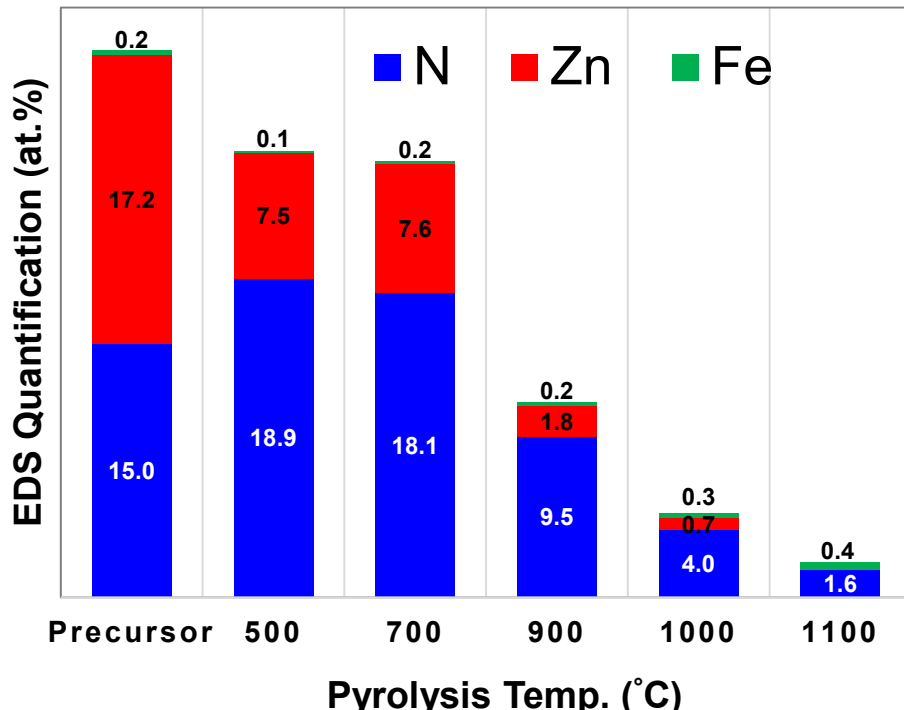


- **Highlight:** ORR activity correlated with atomically dispersed iron, (AD)Fe, rather than particulate Fe
- Small Fe clusters → spectator species

$\text{Fe}_{1.5}\text{Zn}_{98.5}$ ZIF: *Ex situ* Heat Treatment Series

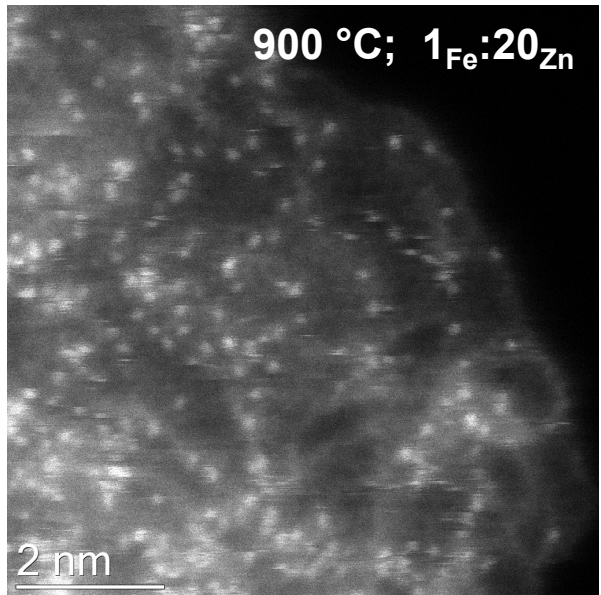


- $\text{Fe}_{1.5}\text{Zn}_{98.5}$ ZIF examined at five heat-treatment temperatures
- Mesoporosity emerging during pyrolysis to 500 °C concomitant with significant loss of Zn
- Very little change in composition or morphology observed between 500-700 °C
- Increasing loss in Zn and N during heat treatment to 900, 1000, and 1100 °C
- Fe content exceeding Zn content only after final heat treatment to 1100 °C

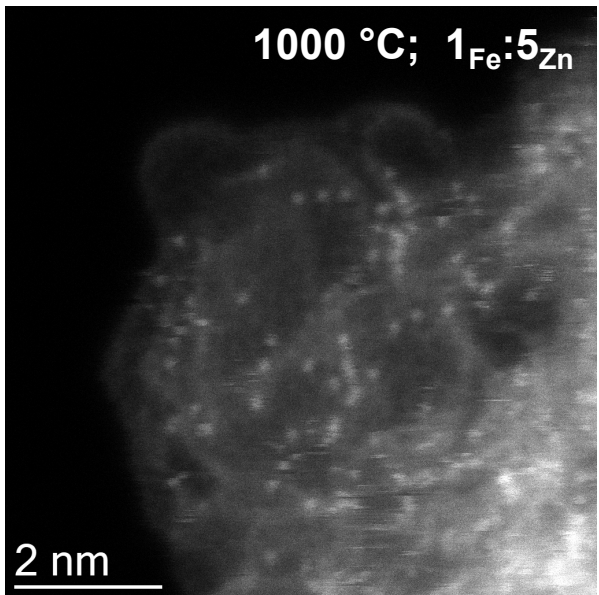


Fe_{1.5}Zn_{98.5} ZIF: *Ex situ* Pyrolysis Series

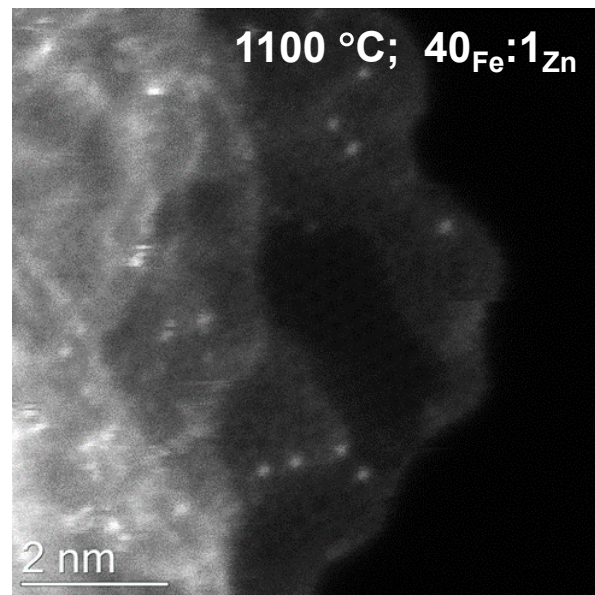
900 °C; 1_{Fe}:20_{Zn}



1000 °C; 1_{Fe}:5_{Zn}



1100 °C; 40_{Fe}:1_{Zn}



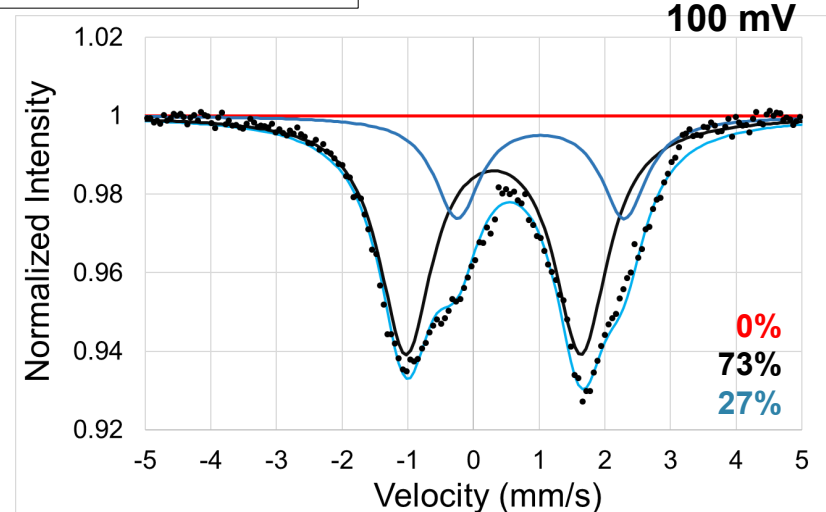
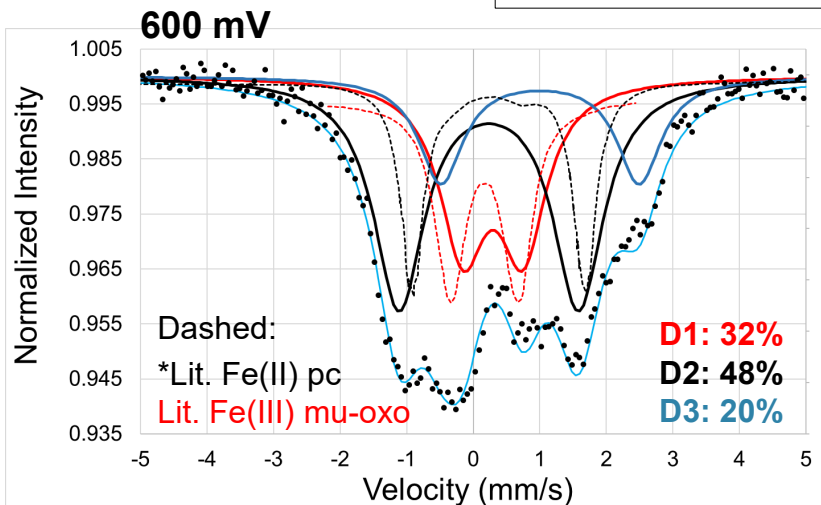
XPS peak fitting (at.%)

Name	Peak BE	900 °C	1000 °C	1100 °C
C (sp ²)	284.6	37.1	49.2	58.9
C (sp ³)	285.1	29.8	28.6	24.4
C-N	286.7	9.1	3.3	1.7
N (pyridine)	398.4	5.1	1.4	0.5
N (amine/nitrile)	399.4	1.3	0.5	0.2
N (pyrrole)	400.8	2.9	1.5	1.1
Fe	710.2	0.1	0.1	0.2
Zn	1022	1.9	0.5	trace

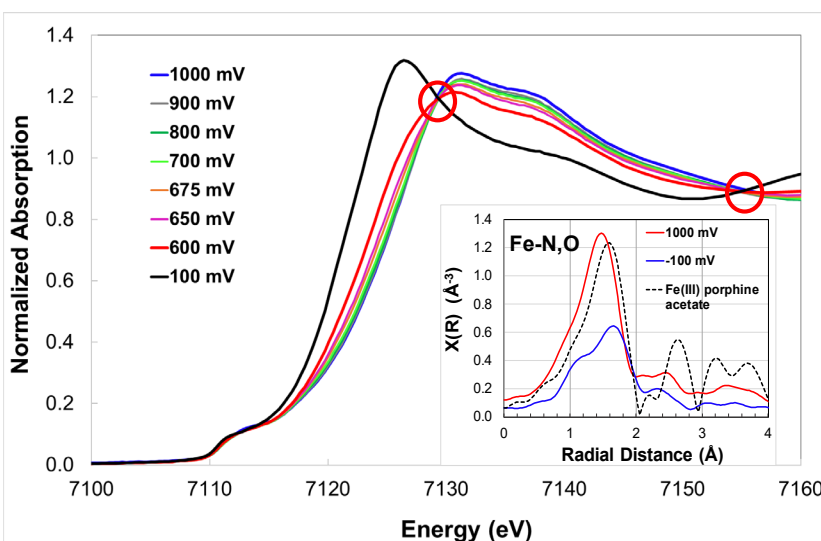
- Increase in graphitization (sp²) observed with annealing from 900-1100°C
- Undesirable loss in pyridinic nitrogen within same temperature range; Fe content stable
- Fe-N moieties likely forming at lower temperatures, as shown by XAFS results, but difficult to observe due to high Zn content
- Temperature-dependent shifts in morphology and speciation determined

Active Site Characterization: *In situ* Mössbauer Spectroscopy

(AD)⁵⁷Fe-N-C (1.5 at% Fe in precursor) in 0.5 M H₂SO₄



*Lit.: Tanaka et al., J. Phys. Chem., 91 (1987) 3799-3807.



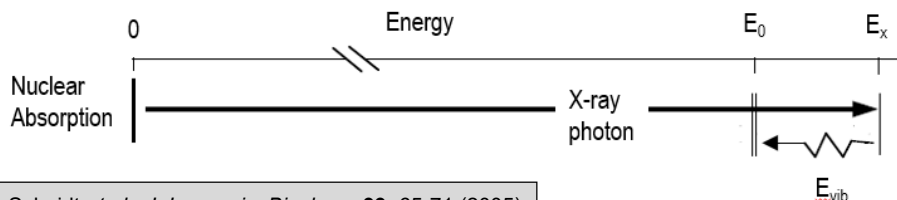
Characteristics	Doublet 1	Doublet 2	Doublet 3
Oxidation State	Fe ³⁺	Fe ²⁺	Fe ²⁺
Spin	5/2	1	2
Fe coordination geometry	Square pyramid or octahedron	Distorted square planar	Octahedral
Content with decreasing potential	Decreases	Increases	Slight dependence (protected)

XAFS showing two major species with the ratio of the two species dependent on potential (isosbestic points); species at high potentials – octahedral, species at low potentials – approximately four-coordinate

NRVS + NO as Surface Probe; (AD)⁵⁷Fe-N-C Catalyst Characterization

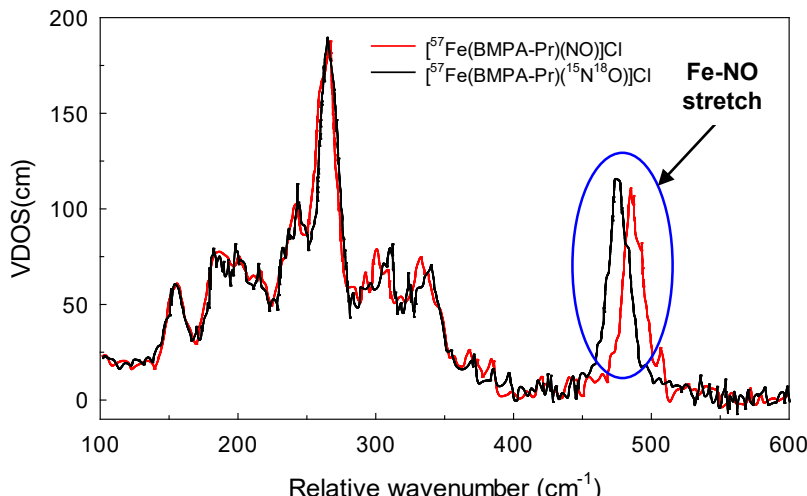
Nuclear resonance vibrational spectroscopy (NRVS): Technique capable of probing vibrational energy levels; specific to samples containing Mössbauer-active nuclei, e.g., ⁵⁷Fe – active site “fingerprints”

Principle: In addition to meeting the Mössbauer-resonant condition, further resonance can occur upon absorption by nucleus of a vibrational energy quantum to state E_x . (Atomic emission of 6.4 keV photon undergoing detection not shown.)



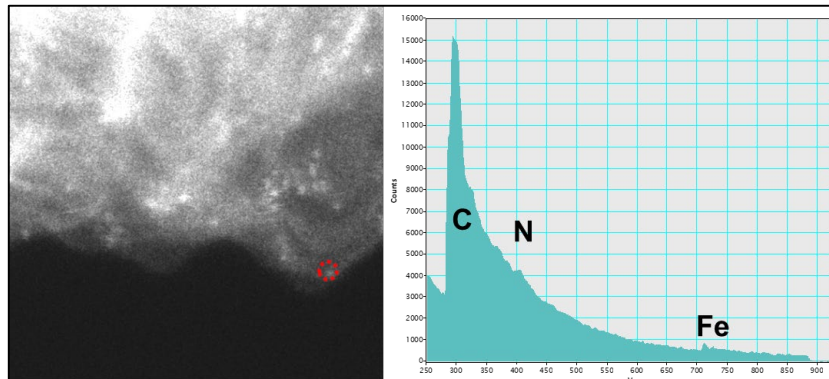
Scheidt *et al.*, *J. Inorganic. Biochem.* **99**, 65-71 (2005)

NO used for probing Fe sites known to activate O₂ in biological systems

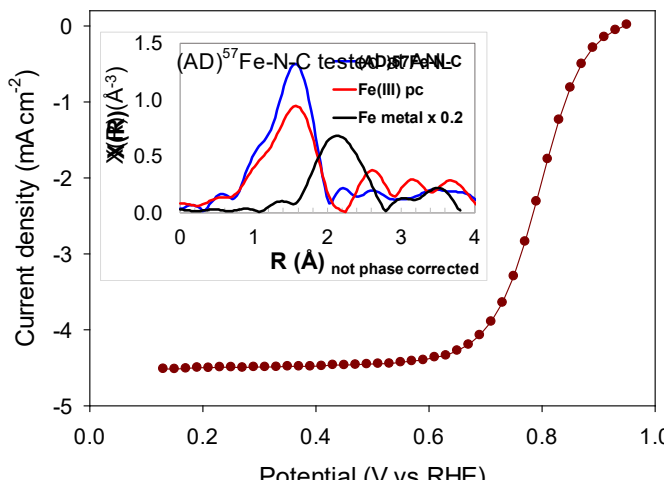


Berto *et al.*, *JACS* **133**, 16714-16717 (2011)

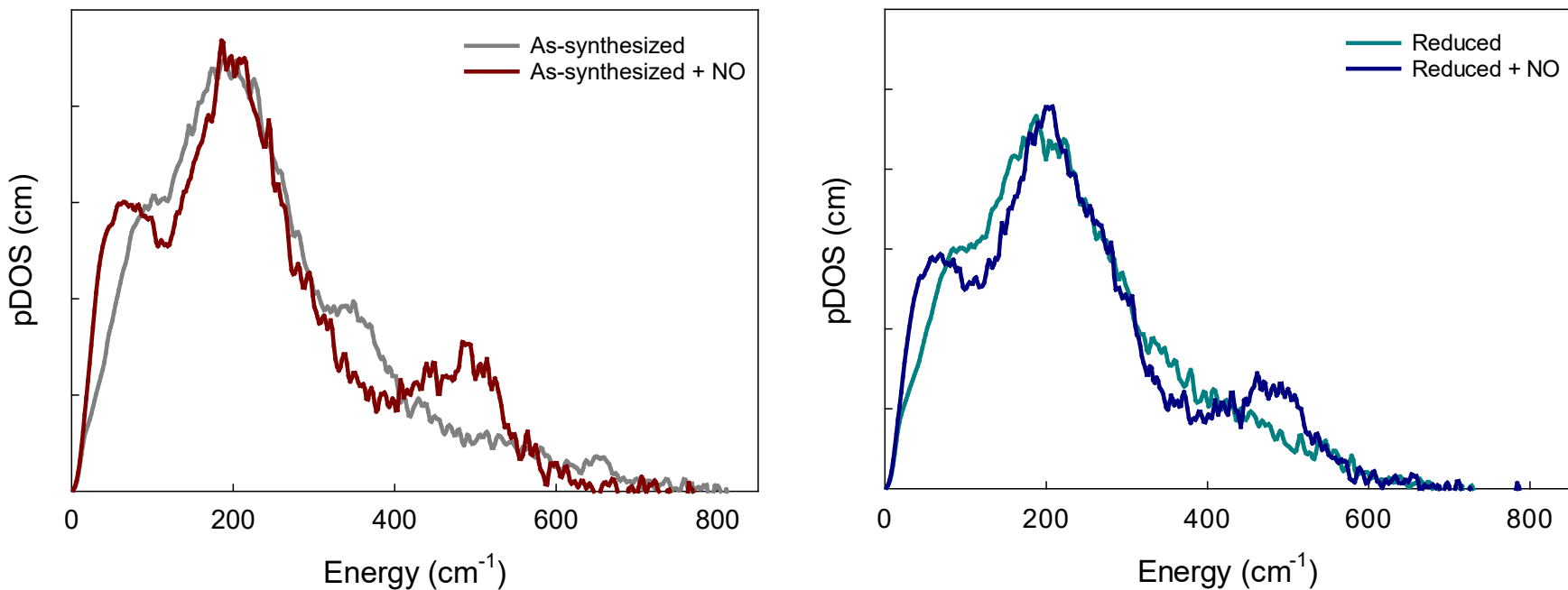
STEM & EELS confirm atomic dispersion of Fe and Fe-N coordination in ⁵⁷Fe-enriched catalyst



ORR activity of ⁵⁷Fe-enriched similar to that of a “regular” (AD)Fe-N-C catalyst



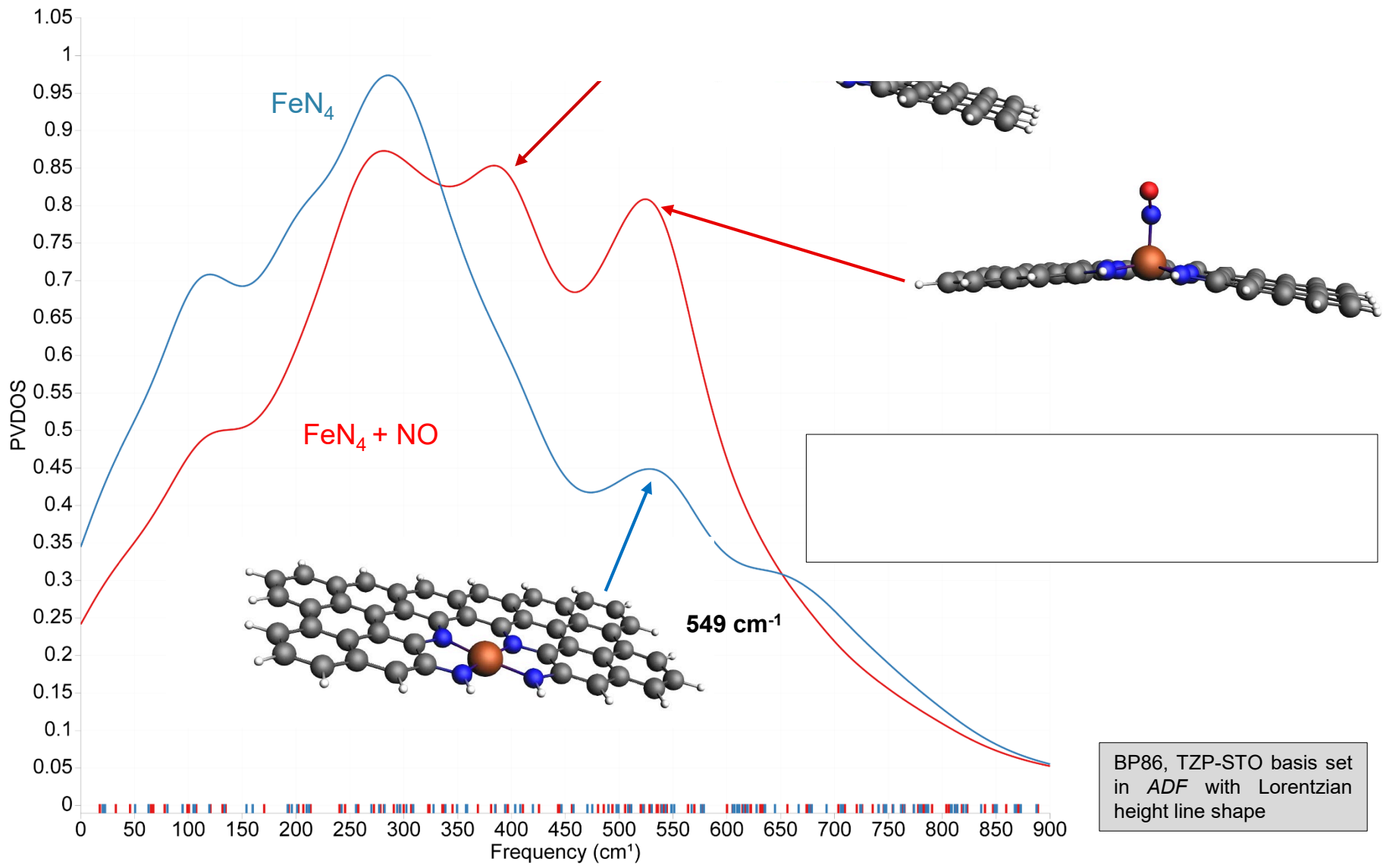
Direct NRVS Detection of Surface Fe Sites in (AD)⁵⁷Fe-N-C



- NRVS used with NO (O_2 analog) as a molecular probe to detect iron sites in (AD)⁵⁷Fe-N-C catalyst; NO appearing to probe both Fe^{3+} and Fe^{2+}
- 400-600 cm⁻¹ – Fe-NO stretch vibration; (i) direct evidence of Fe-NO bond; (ii) broad band suggesting a possibility of more than one FeN_x moiety
- 0-200 cm⁻¹ – acoustic mode involving overall translation of the entire catalyst; NO adsorption possibly modifying whole acoustic mode of Fe

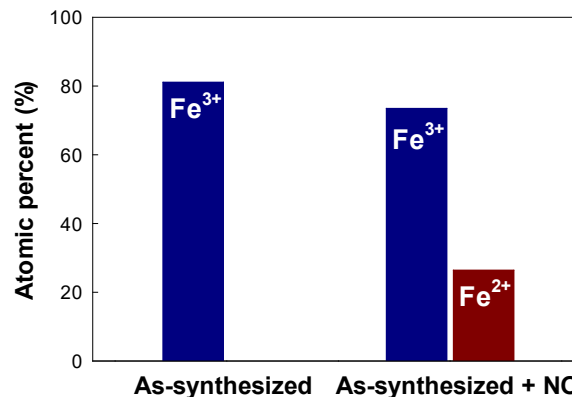
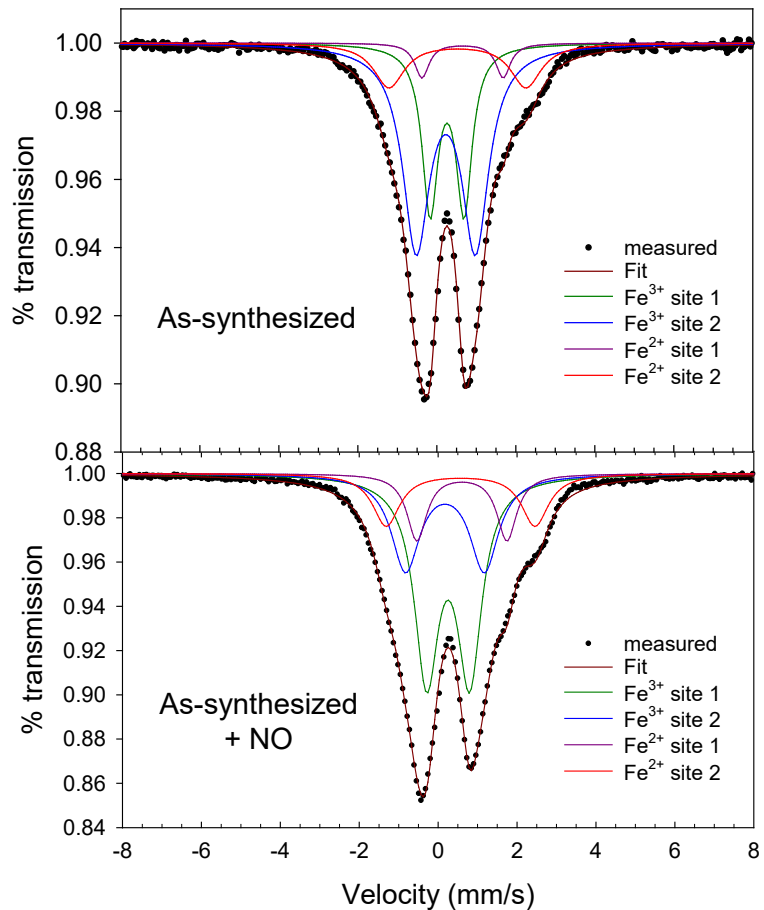
Highlight: First evidence of NO probe binding to both Fe^{3+} and Fe^{2+} surface sites of a PGM-free catalyst

DFT Calculation: NRVS with NO Probe Molecule



Highlight: FeN_4 signatures most consistent with NRVS experiment

(AD)⁵⁷Fe-N-C Catalyst: Mössbauer Spectroscopy



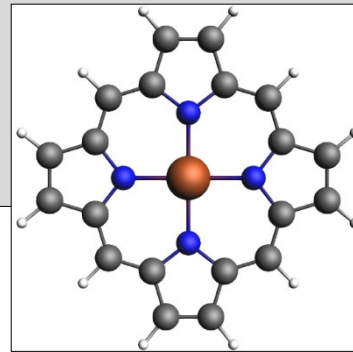
DFT Database Isomer Shifts and Quadrupole Splitting in Mössbauer spectra

Example:

porphyrinic FeN_4

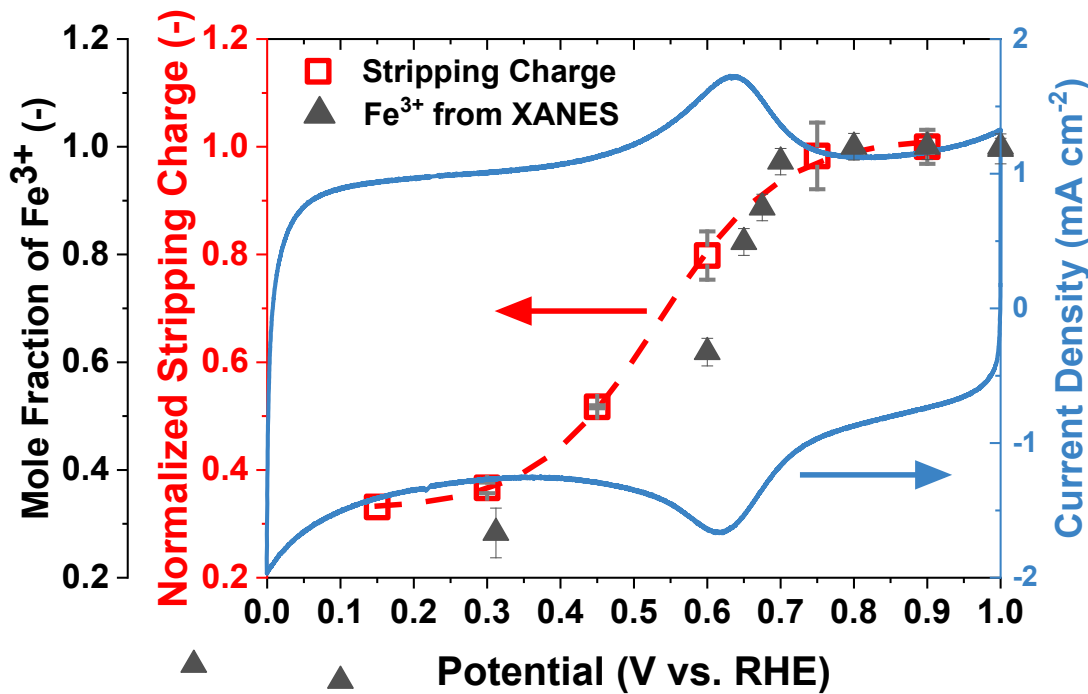
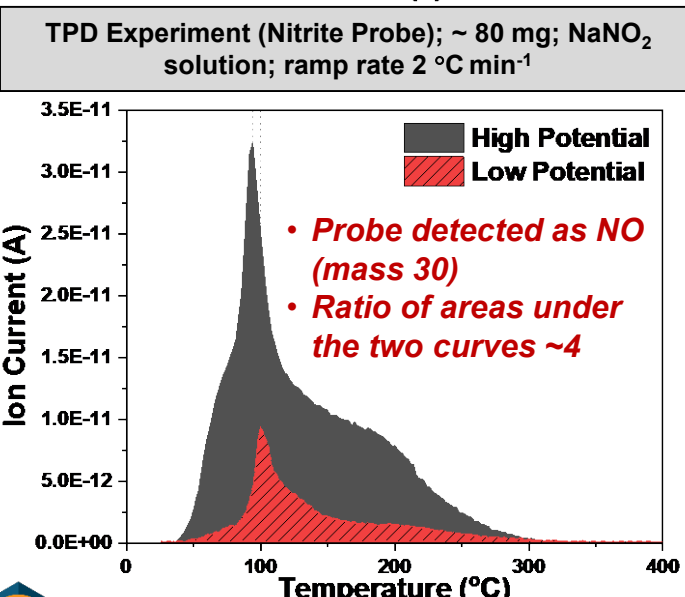
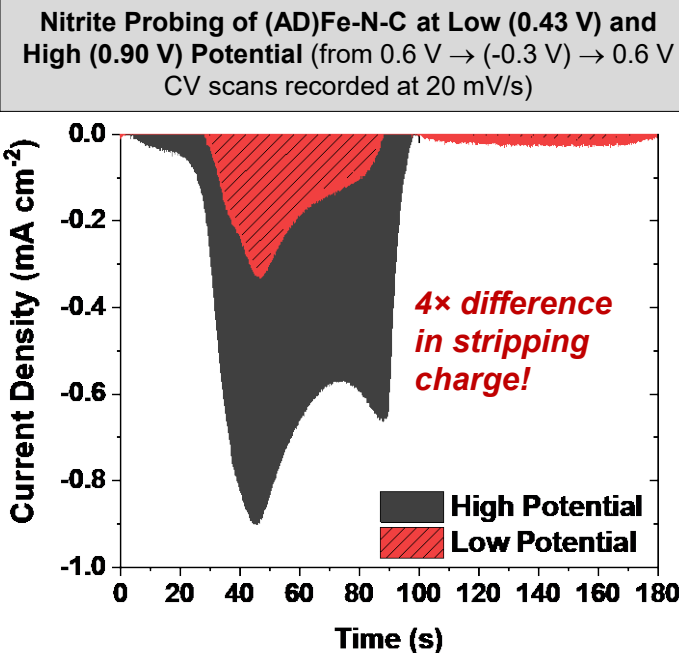
IS_{DFT} : 0.56 mm/s

QS_{DFT} : 3.01 mm/s



- NO (an O_2 analog) inducing changes in quadrupole splitting in Mössbauer spectra of both Fe^{3+} and Fe^{2+} assigned sites
- NO interacting with Fe^{3+} and Fe^{2+} ; a decrease in $\text{Fe}^{3+}/\text{Fe}^{2+}$ ratio observed upon NO treatment
- DFT database of the isomer-shift and quadrupole-splitting values as a function of structure (with and without NO) underway – coupled with vibrational calculations for identification

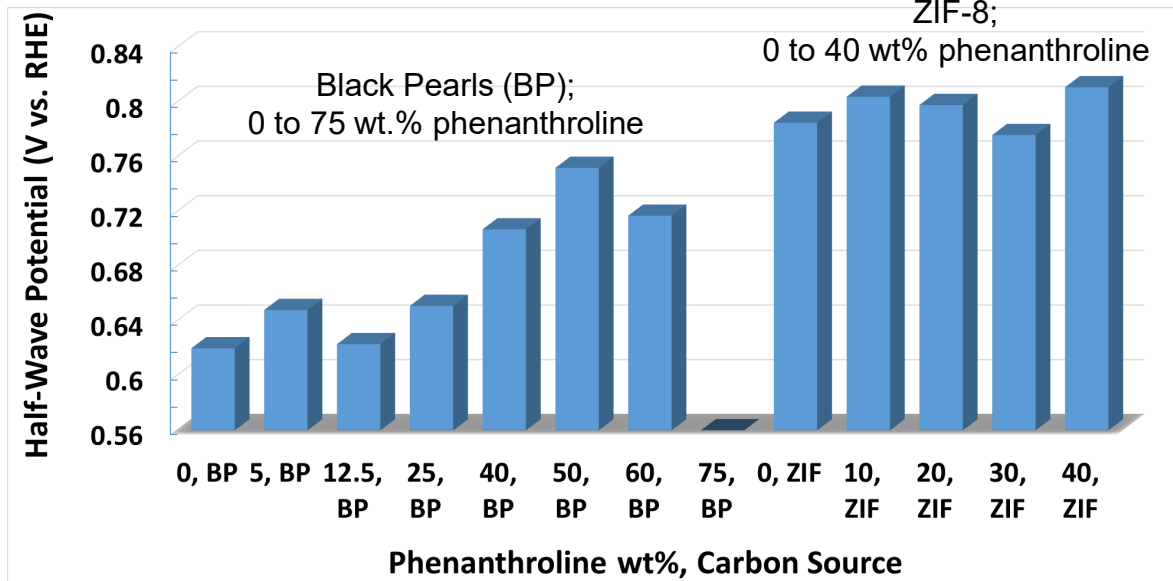
Molecular Probes: Effect of Potential on ORR Poisoning & Stripping Charge



- Stripping charge of the nitrite probe adsorbed at 0.90 V (ca. $1.3 \cdot 10^{13}$ sites/ cm^2), approximately four times higher than at 0.43 V (ca. $3.0 \cdot 10^{12}$ sites/ cm^2); confirmed by TPD data
- DFT calculations implying NO attachment to available Fe, as well as some local epoxides
- Calculations also suggesting no NH_3 binding to edge FeN_4 ; consistent with assumed formation of NH_4^+
- Similar trend for the charge density when poisoned at different potentials and mole fraction of $\text{Fe}^{2+}/\text{Fe}^{3+}$ obtained from XANES linear combination

High-throughput Synthesis: Effect of Carbon Source and Fe Content

0.5 wt% Fe

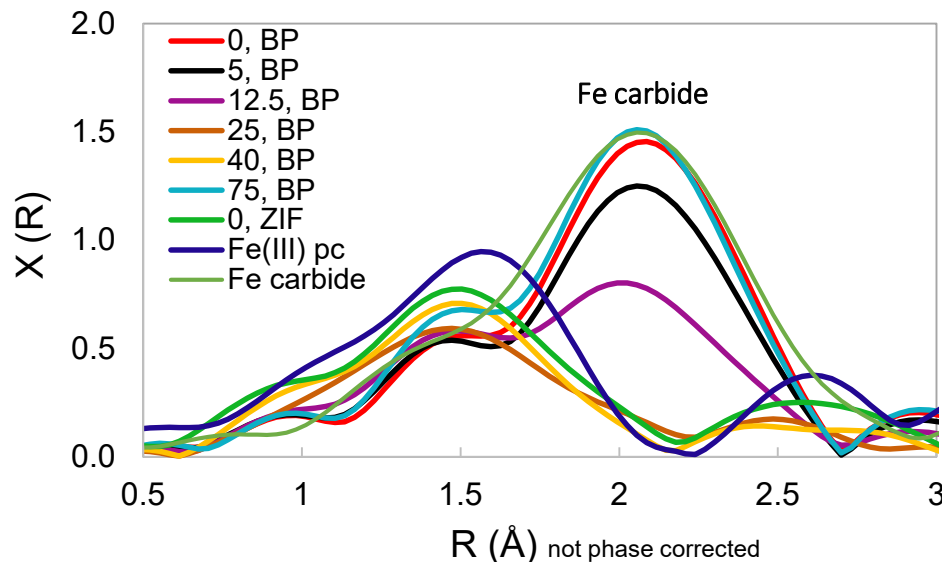


Catalyst synthesis:

Iron acetate; precursors ball-milled, heat-treated at 1050 °C (5 °C/min) in Ar for 1 h; heat-treated at 950 °C in NH₃ for 5 min.

RDE evaluation of ORR activity:

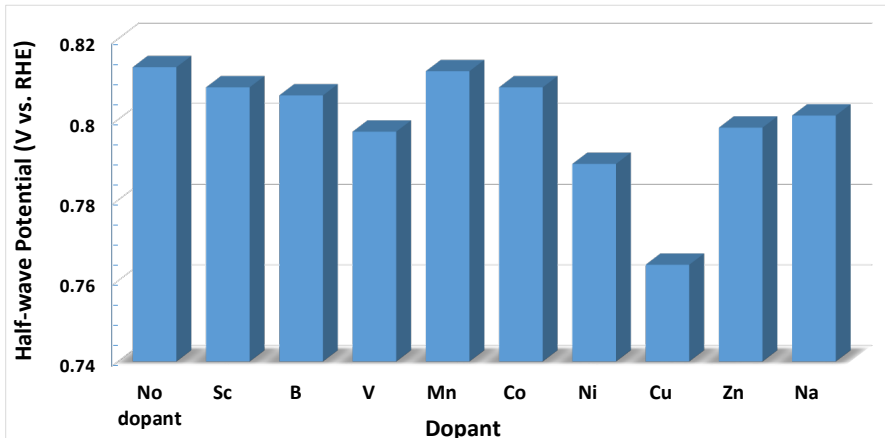
0.6 mg_{cat}/cm²
O₂-saturated 0.5 M H₂SO₄
steady-state current measurements
Carbon-rod counter electrode



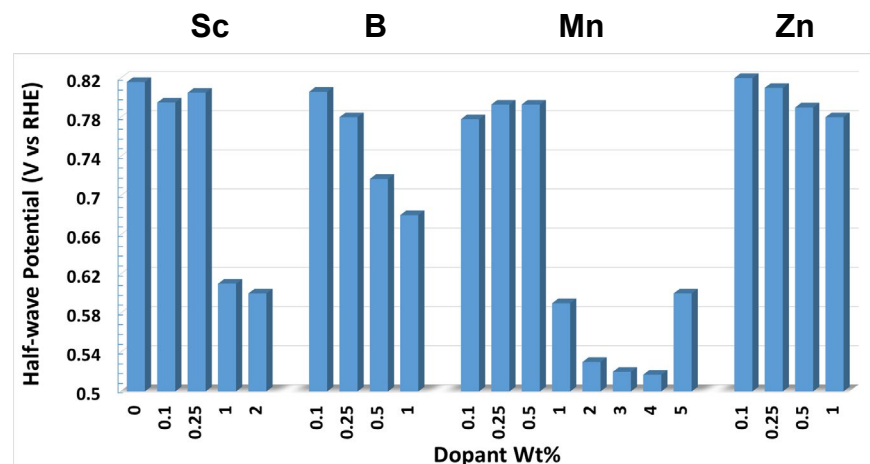
- Iron carbide formed in the absence of phenanthroline or ZIF in precursor; exclusively FeN_x formed with ZIF in precursor or 25-60% phenanthroline with BP carbon; high phenanthroline contents also promoting carbide formation
- Highest ORR activity with ZIF vs. BP carbon source and phenanthroline content of 40 wt.% ($E_{1/2} = 0.81$ V)

High-throughput Synthesis: Effect of Dopant Content on Fe, Mn vs. Fe

0.9 wt.% Fe, ZIF, 40 wt.% phenanthroline,
0.1 wt.% second-metal dopant

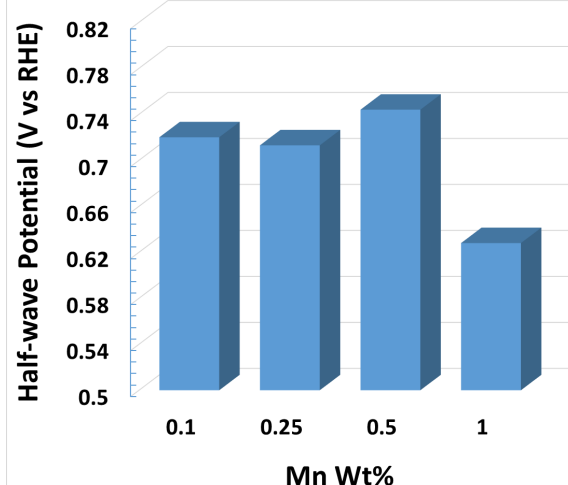


0.8 wt.% Fe, ZIF, 40 wt.% phenanthroline



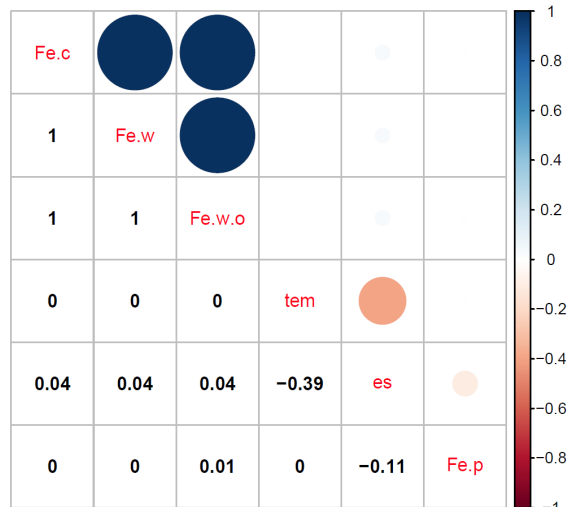
- Studied effect of Fe loading from 0.05 wt.% to 1.0 wt.% and effect of Fe salt for ZIF, 40 wt.% phenanthroline material:
 - ✓ 0.8 wt.% Fe using Fe acetate showing highest ORR activity
 - ✓ Carbide content increasing with increasing Fe content above 0.3 wt.% (determined by EXAFS)
- Studied effect of adding a dopant metal and dopant metal loading:
 - ✓ 0.1 wt.% Zn dopant enhancing ORR activity of catalyst derived from 0.8 wt.% Fe, 40 wt.% phenanthroline, balance ZIF
- Mn-based catalysts exhibiting lower ORR activity than Fe-based catalysts at all loadings tested

0 wt.% Fe, ZIF,
40 wt.% phenanthroline



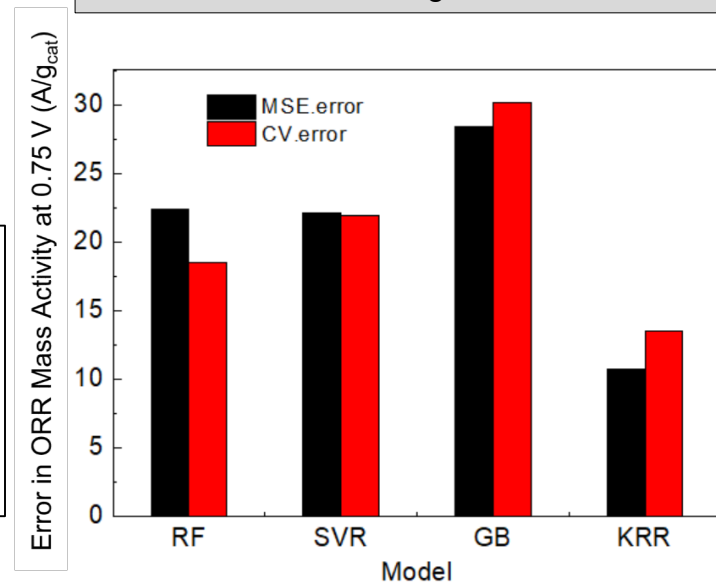
Machine Learning Capability Development

High-Throughput Activity:Parameter Correlation



Fe.c: Fe concentration
Fe.w: at.% Fe w/ H_2O
Fe.w.o: at.% Fe w/o H_2O
es: ORR mass activity at 0.75 V ($A/g_{catalyst}$)
tem: pyrolysis temperature
Fe.p: Fe precursor

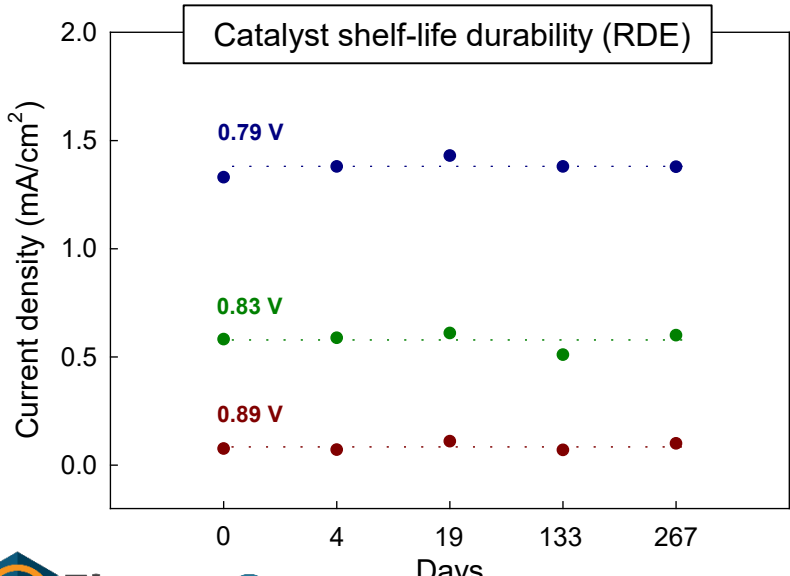
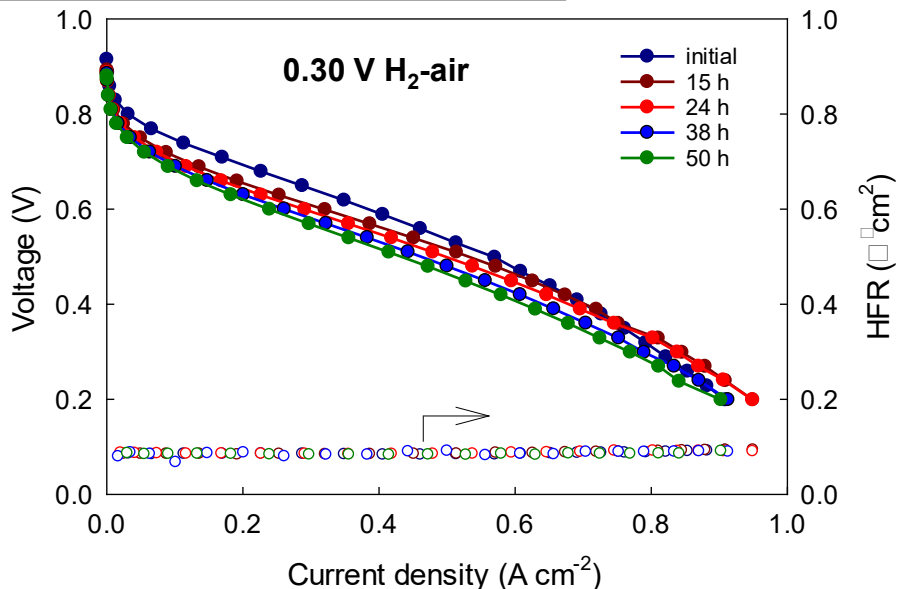
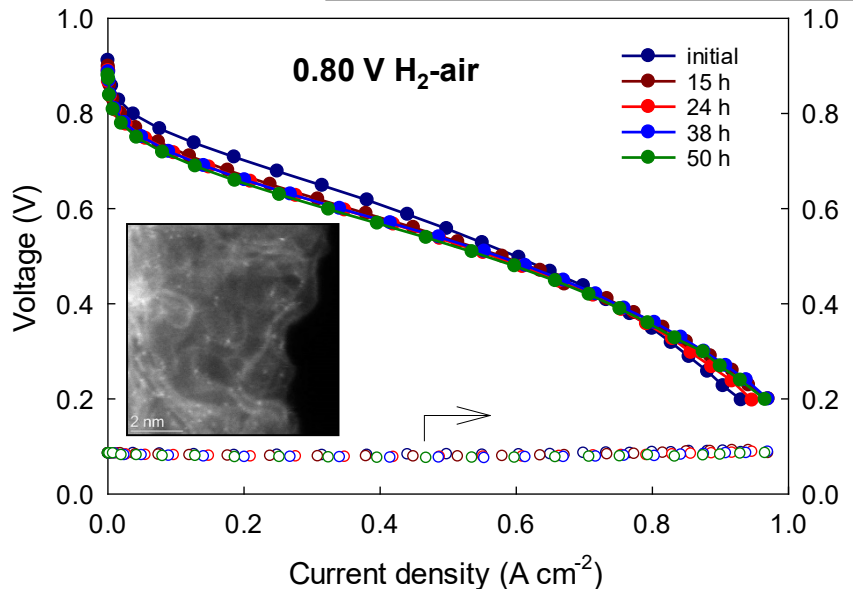
Mean Squared Error and Cross Validation Errors for Tested Regression Models



- **Highlight:** Kernel Ridge Regression (KRR) approach shown to best capture high-throughput experimental data
- First iteration of *Adaptive Design* applied – decreased temperature and modified precursor ratios prescribed for activity optimization
- Go/No-Go goal **accomplished**
- DFT database of dopants calculations converged; input to learning models (stretch goal for FY19)

(AD)Fe-N-C Catalyst: H₂-Air Fuel Cell Performance and Durability

Anode: 0.2 mg_{Pt} cm⁻² Pt/C H₂, 200 sccm, 1.0 bar H₂ partial pressure; Cathode: 4.0 mg cm⁻² (AD)Fe-N-C 1.5 at.% Fe catalyst, air, 200 sccm, 1.0 bar air partial pressure; Membrane: Nafion® 212; Cell: 80 °C

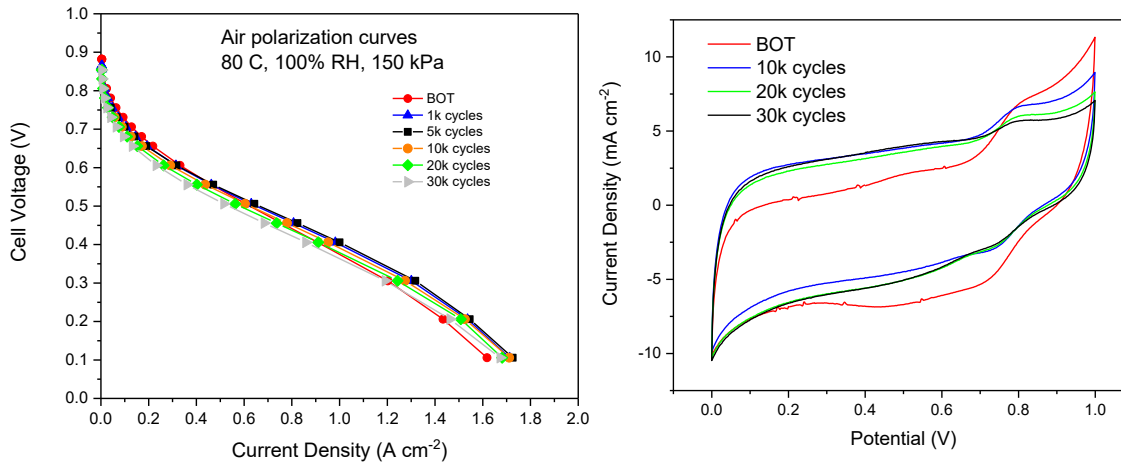


- **Highlight:** Much improved fuel cell performance durability relative to that of catalysts synthesized using individual Fe, N, and C precursors
- Better durability after holds at 0.80 V than at 0.30 V, possibly due to lower H₂O₂ generation
- No loss in ORR activity of catalyst stored for nearly 9 months in ambient air

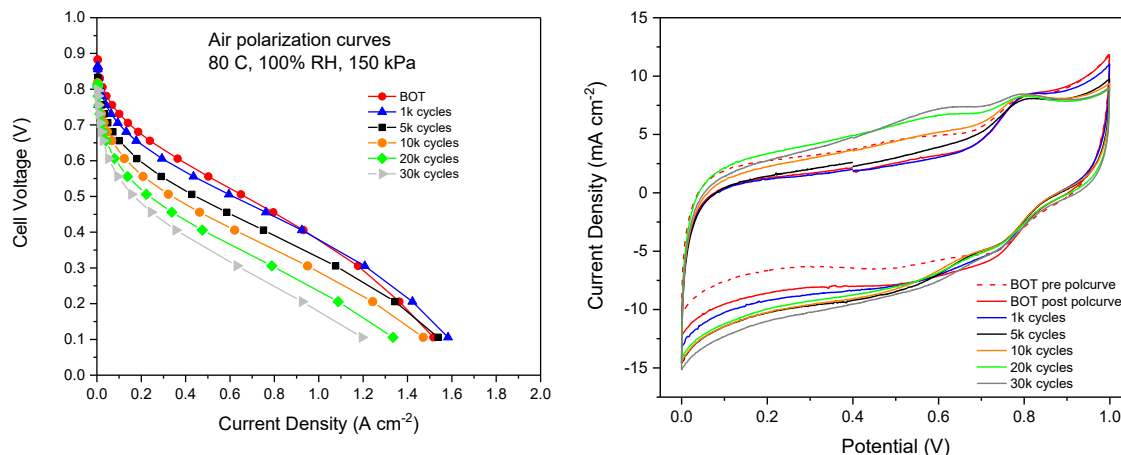
(AD)Fe-N-C Accelerated Stress Tests in Nitrogen and Air

Anode: 0.2 mg_{Pt} cm⁻² Pt/C H₂, **Cathode:** (AD)Fe_{1.5}-N-C catalyst, **Membrane:** Nafion® 211; **Polarization curve conditions:** 80 °C, 100% RH, 150 kPa absolute pressure. Flow rates anode: 1.5 slpm; cathode: 3.3 slpm.

Cycling between 0.60 V and 0.95 V, nitrogen



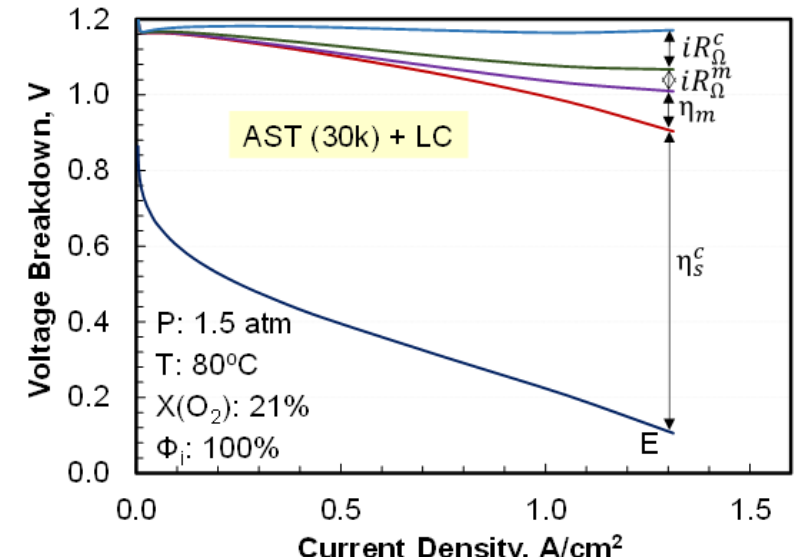
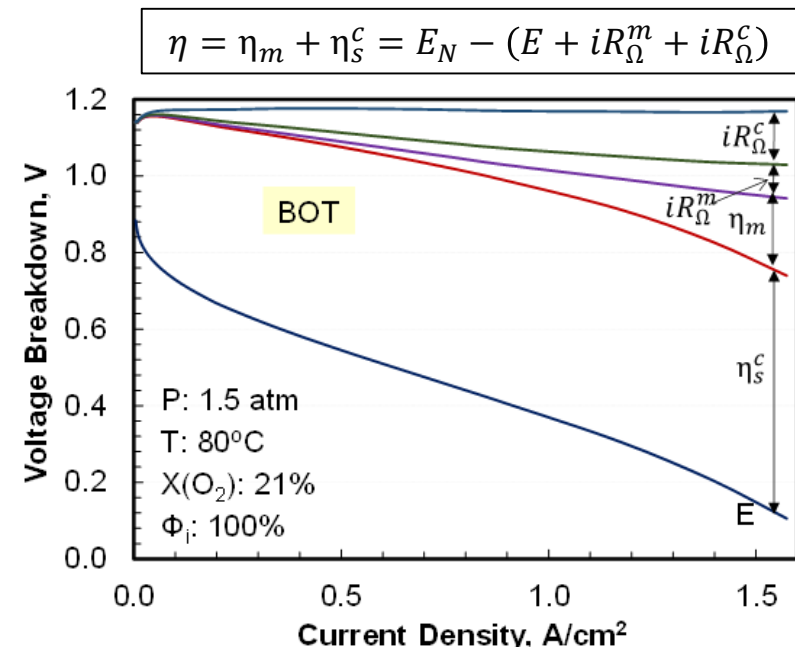
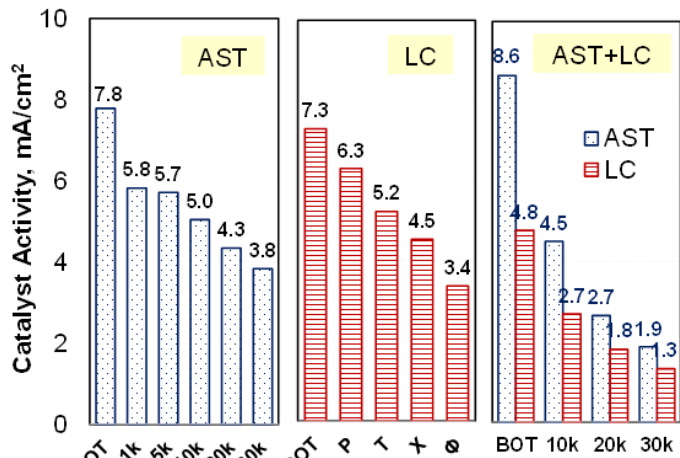
Cycling between 0.60 V and 0.95 V, air



- Accelerated stress test (AST) cycling with air supplied to cathode resulting in much higher performance loss than when cycling in nitrogen
- Despite large loss in performance in the kinetic region when cycling in air, the Fe³⁺/Fe²⁺ voltammetric signature (reversible redox couple) remaining relatively unchanged; in need of understanding in the context of suggested key role of atomically dispersed Fe sites in ORR
- Second reversible redox couple appearing over the duration of the AST at lower potentials than that of the Fe³⁺/Fe²⁺ couple

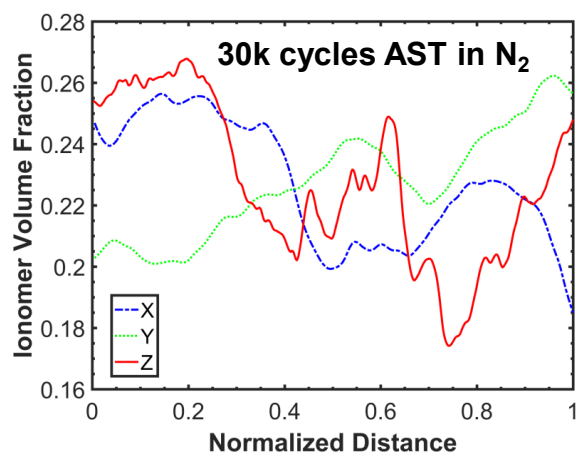
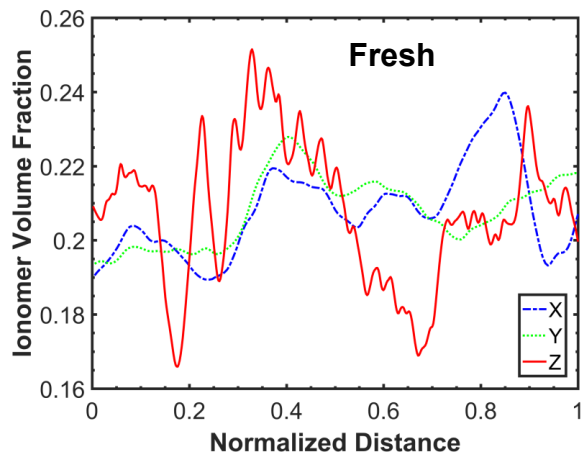
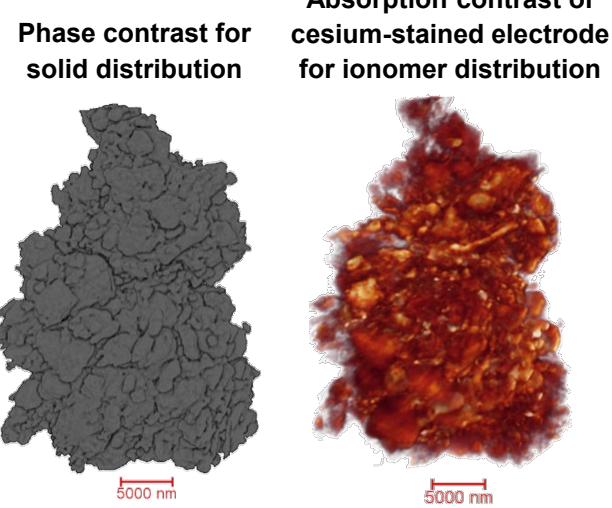
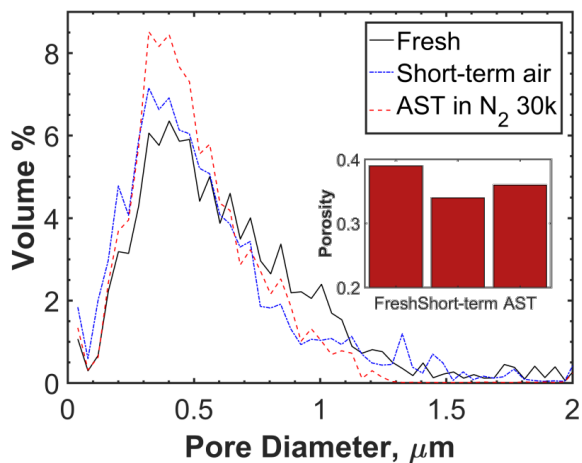
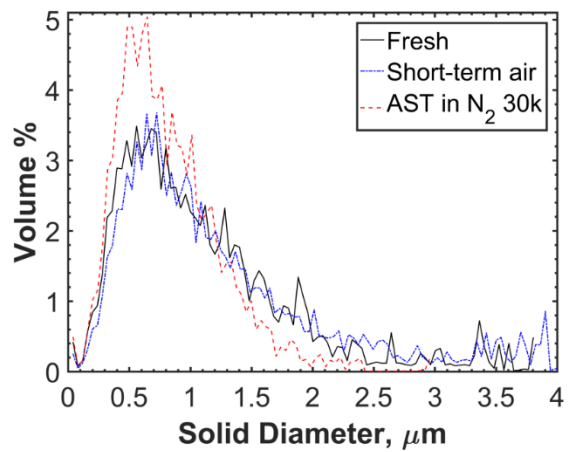
(AD)Fe-N-C Accelerated Stress Tests in Nitrogen and Air

- Cell voltage increasing in first 5,000 cycles due to decreases in cathode catalyst layer ohmic resistance (iR_{Ω}^c) and mass transport overpotential (η_m); > 40% decrease in cathode sheet resistance
- Cell voltage decrease from 5,000 to 30,000 cycles caused by increase in ORR overpotential ($\Delta\eta_s^c = 30$ mV)
- Load cycling in air causing an additional 125 mV increase in $\Delta\eta_s^c$ and a 20 mV increase in η_m
- Catalyst activity decreasing by ~50% after 30,000 AST cycles in N_2 ; no increase in sheet resistance indicating no effect of catalyst degradation products on ionomer conductivity
- > 75% loss in active sites causing < 20% increase in local O_2 transport resistance (R_{cf}), much lower than observed with low-PGM catalyst layers



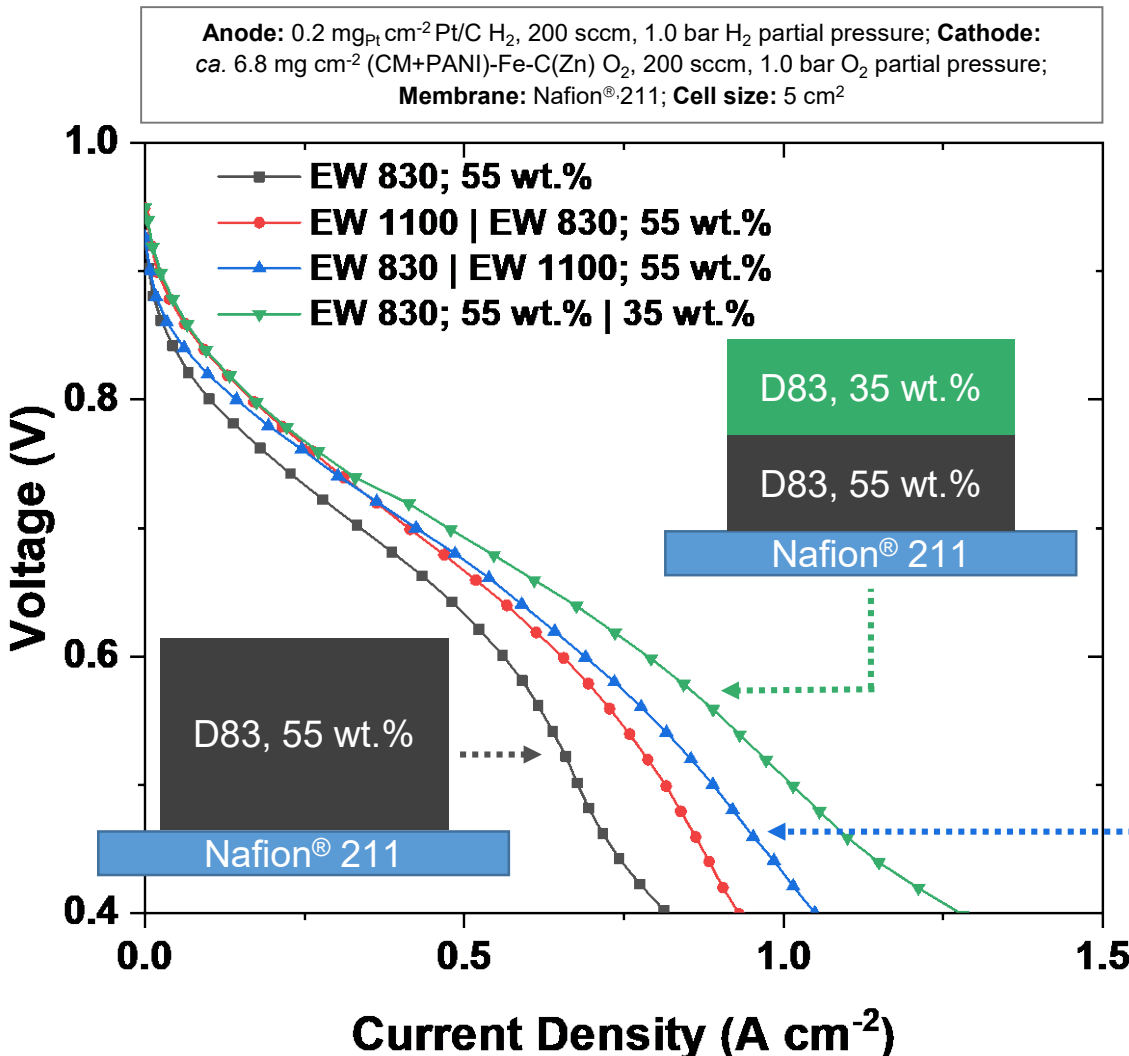
Effect of AST Cycling on (AD)Fe-N-C Electrode Morphology

Phase and Absorption Contrast in Nano X-ray Computed Tomography



Morphology of the solids, pore diameter, and ionomer spatial distribution, not significantly impacted by short-term load cycling in air or 30,000 AST cycles in nitrogen

Layered PGM-Free Electrode for Improved Mass Transport



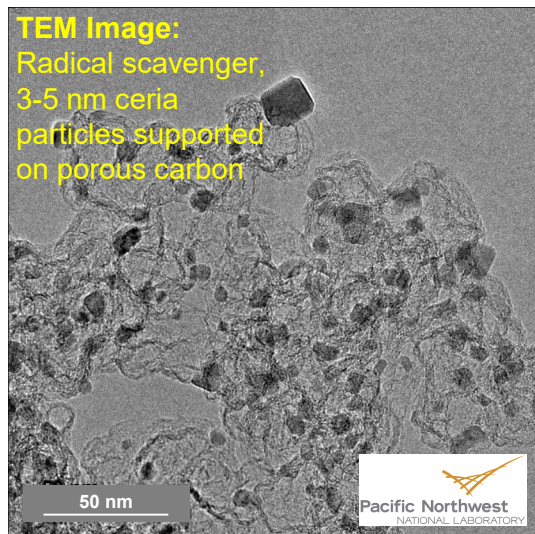
- In thick electrodes, lower current density generated near the MPL due to mass-transport resistance and flooding

Komini Babu et al., JECS 164, F1037-F1049 (2017)

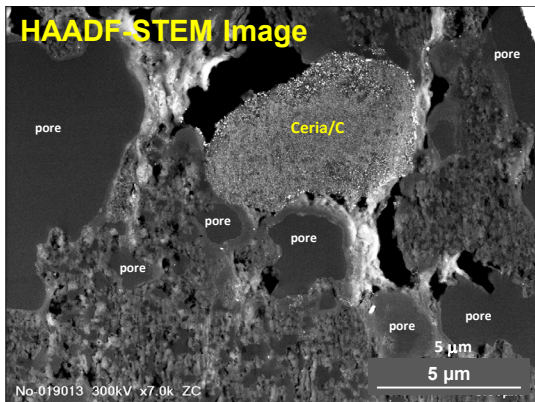
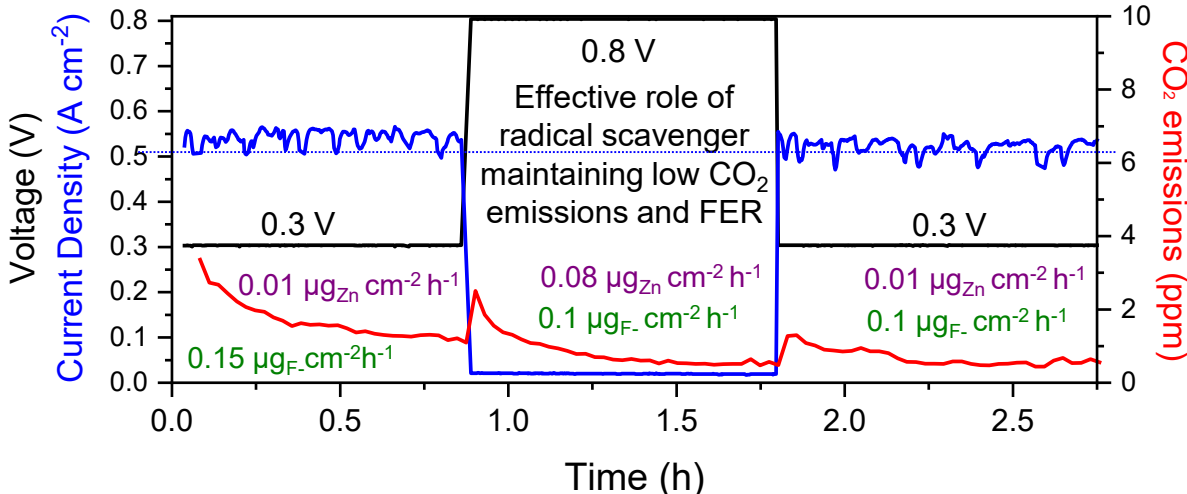
- Decreasing hydrophilicity in the catalyst layer near the MPL expected to result in improvements in water management and increased catalyst utilization

Highlight: Improved electrode performance in the layered structure observed with I/C gradient due to water management and possibly, better interface with the MPL

Effect of Radical Scavenger Addition to (CM+PANI)-Fe-C(Zn)

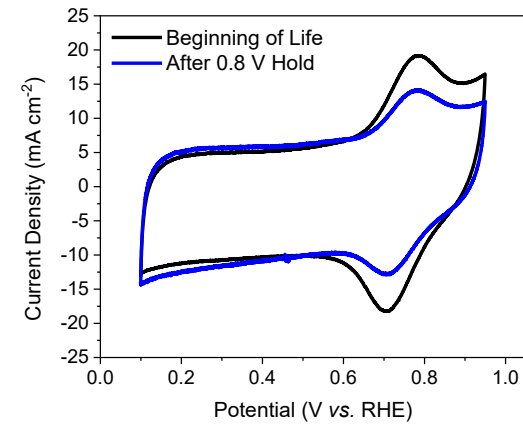
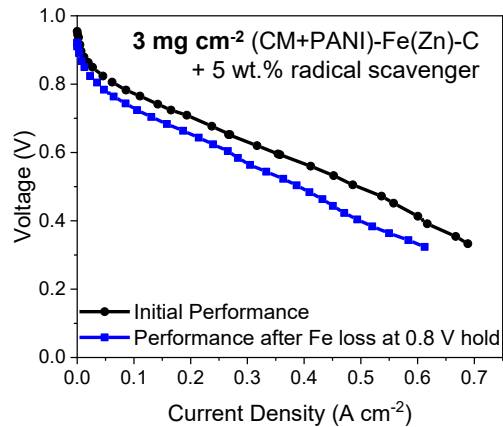


Anode: 0.2 $\text{mg}_{\text{Pt}} \text{cm}^{-2}$ Pt/C H₂, 200 sccm, no backpressure; **Cathode:** ca. 3 mg cm^{-2} (CM+PANI)-Fe-C(Zn) + 5 wt. % radical scavenger, air, 500 sccm, no backpressure; **Cell:** Nafion®211; 5 cm^2 ; 80 °C; 100% RH, constant voltage: 0.3 V, 0.8 V



Radical scavenger physically mixed with (CM+PANI)-Fe-C-(Zn) in catalyst layer

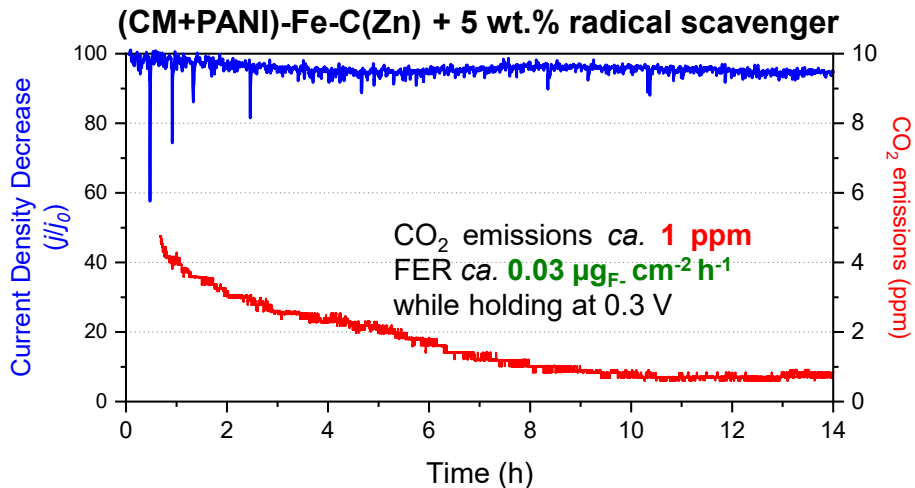
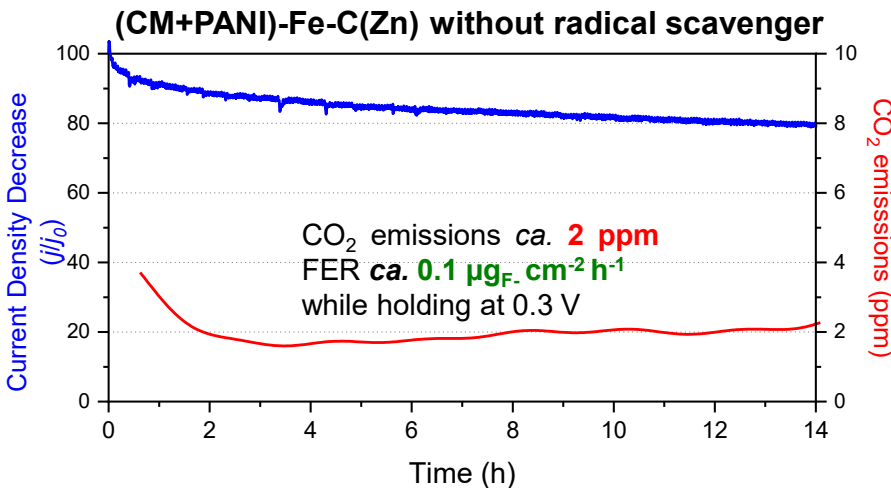
Anode: 0.2 $\text{mg}_{\text{Pt}} \text{cm}^{-2}$ Pt/C H₂, 200 sccm, 1.0 bar H₂ partial pressure for polarization plots; **Cathode:** ca. 3 mg cm^{-2} (CM+PANI)-Fe-C(Zn) + 5 wt. % radical scavenger, air, 500 sccm, 1.0 bar air partial pressure for polarization plots; **Cell:** Nafion®211; 5 cm^2 ; 80 °C; 100% RH



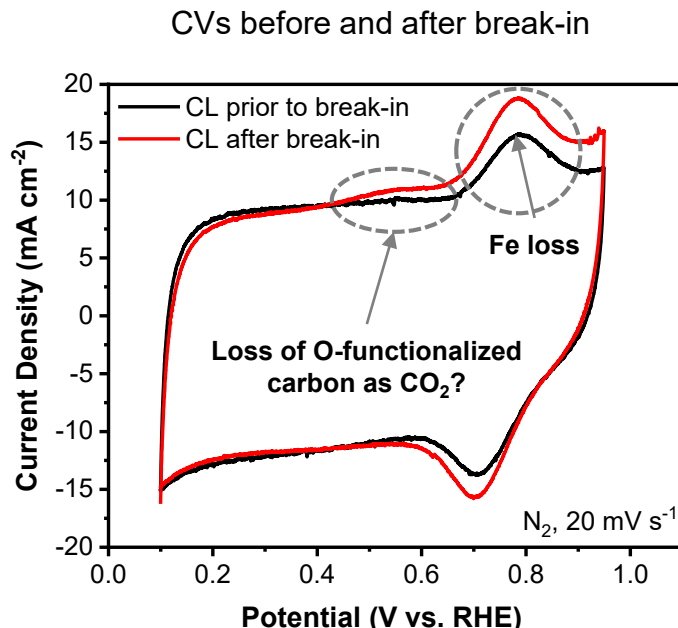
After 0.8 V hold, significant Fe loss as observed causing performance loss, yet FER and CO₂ emissions remain low

(CM+PANI)-Fe-C(Zn) Catalyst Durability with and without Radical Scavenger

Anode: 0.2 $\text{mg}_{\text{Pt}} \text{cm}^{-2}$ Pt/C H₂, 200 sccm, no backpressure; Cathode: ca. 4.5 mg cm^{-2} (CM+PANI)-Fe-C(Zn) or ca. 3.0 mg cm^{-2} (CM+PANI)-Fe-C(Zn) + 5 wt.% radical scavenger, air, 500 sccm, no backpressure; Cell: Nafion® 211; 5 cm^2 ; 80 °C; 100% RH, constant voltage: 0.3 V

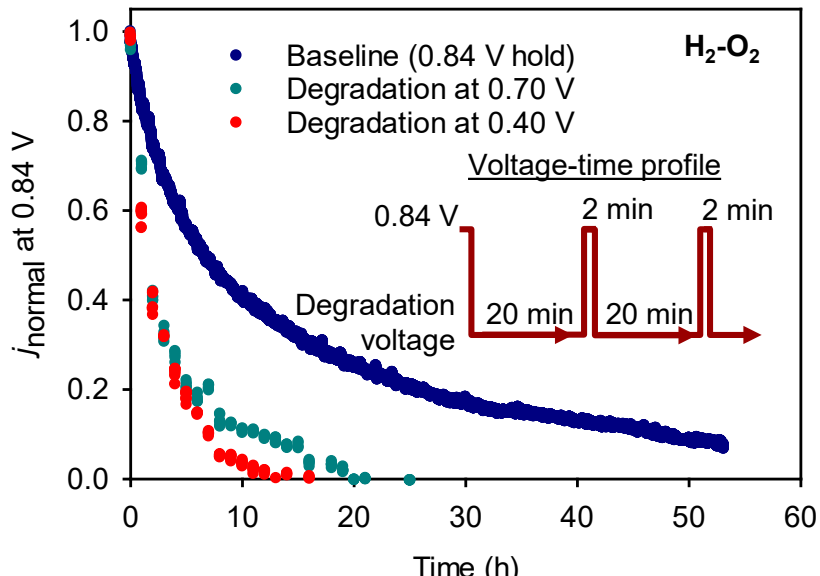


- Initial CO_2 emissions most likely due to removal of oxygen-functionalized carbons
- Stable current densities during 0.3 V hold, lower CO_2 emissions, and nearly negligible FER demonstrate effect of radical scavenger
- During break-in Fe and Zn detected in effluent water ($0.09 \mu\text{g}_{\text{Fe}} \text{cm}^{-2} \text{h}^{-1}$ and $0.56 \mu\text{g}_{\text{Zn}} \text{cm}^{-2} \text{h}^{-1}$), but CO_2 emissions and FER remain relatively low



(CM+PANI)-Fe-C(Zn) Performance Durability Testing in H₂-O₂ Fuel Cell

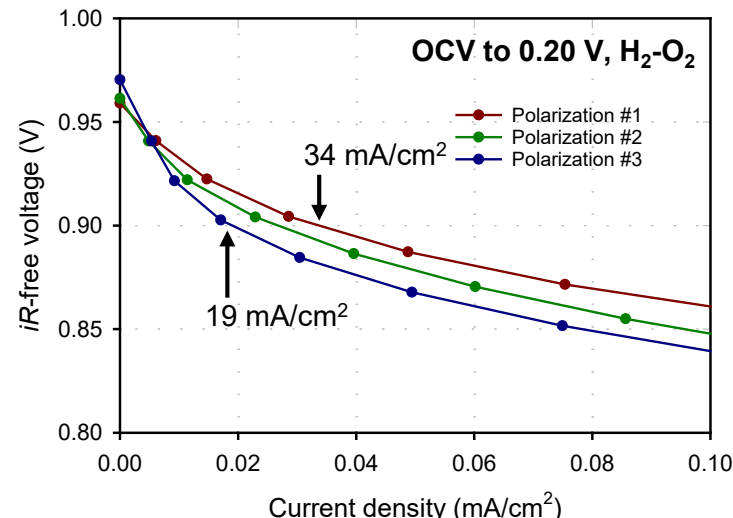
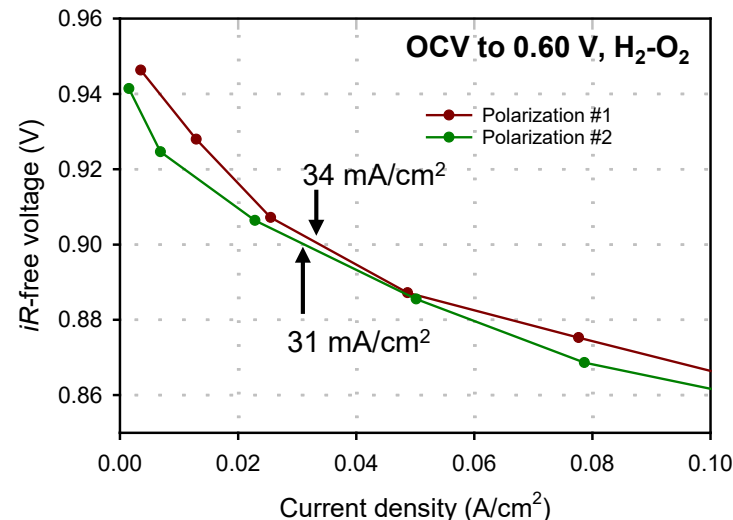
Anode: 0.2 mg_{Pt} cm⁻² Pt/C H₂, 200 sccm, 1.0 bar H₂ partial pressure; **Cathode:** ca. 4.8 mg cm⁻², CM-PANI-Fe-C(Zn), Aquivion® D83 55 wt%, 200 sccm, 100% RH, 1.0 bar O₂ partial pressure; **Membrane:** Nafion® 211; **Cell:** 5 cm²



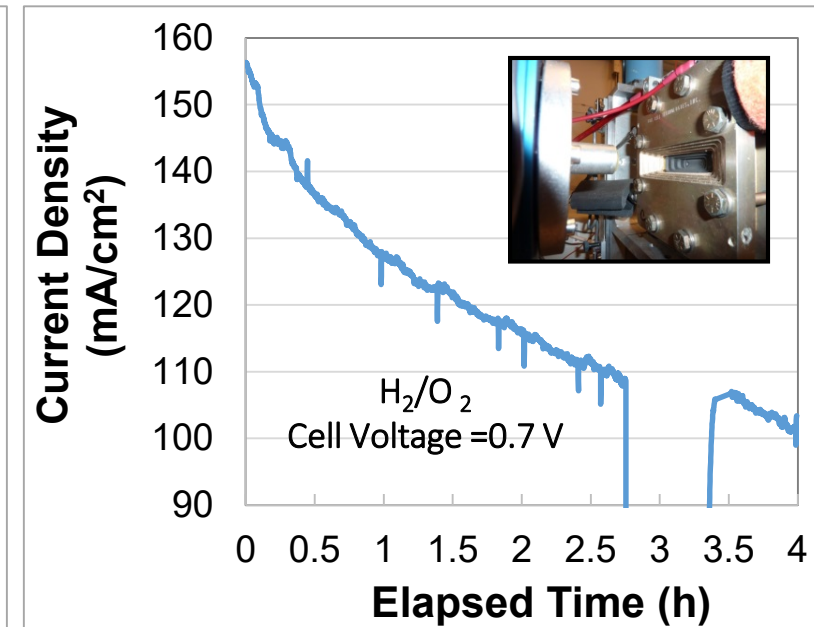
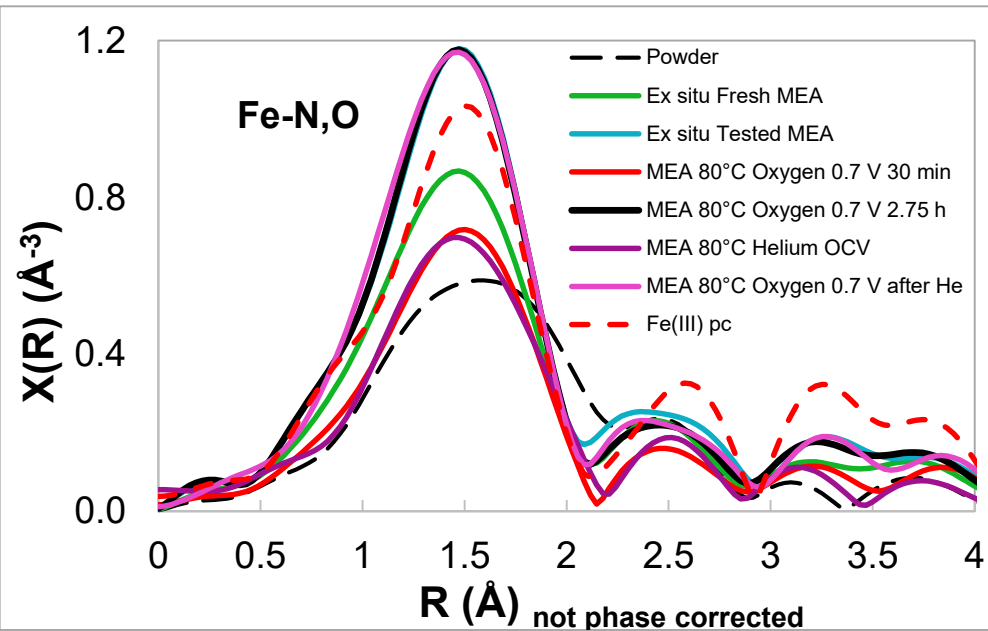
X. Yin and P. Zelenay, ECS Trans. 2018, 85, 1239-1250

- Performance loss in H₂-O₂ fuel cell accelerated at low voltages (high current densities)
- 10% loss in current density at 0.90 V (*iR*-corrected) after two polarization cycles between OCV and 0.60 V
- 44% loss in current density at 0.90 V (*iR*-corrected) after three polarization cycles between OCV and 0.20 V

Anode: 0.2 mg_{Pt} cm⁻² Pt/C H₂, 200 sccm, 1.0 bar H₂ partial pressure; **Cathode:** ca. 6.8 mg cm⁻², CM-PANI-Fe-C(Zn), Aquivion® D83 55 wt%, 200 sccm, 100% RH, 1.0 bar O₂ partial pressure; **Membrane:** Nafion® 211; **Cell:** 5 cm²

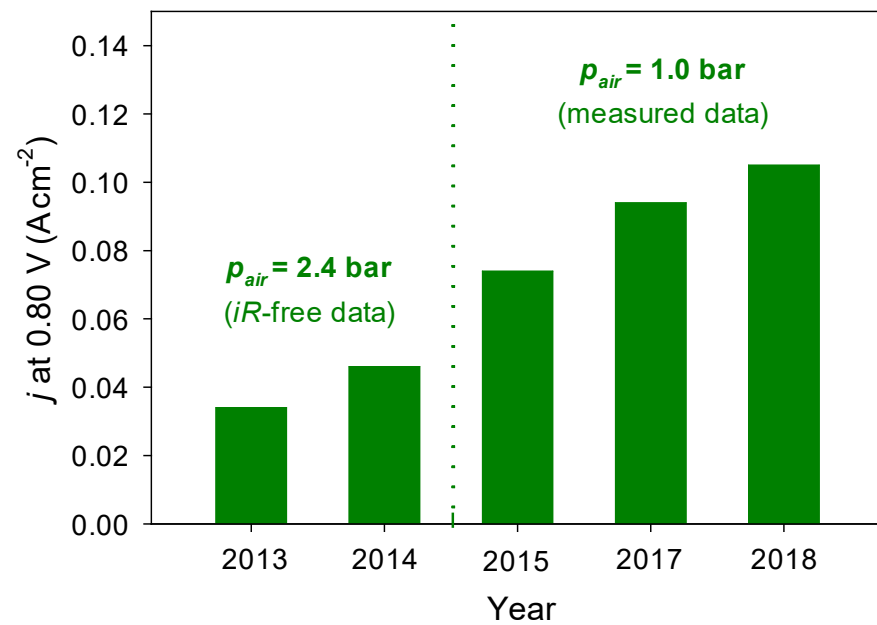
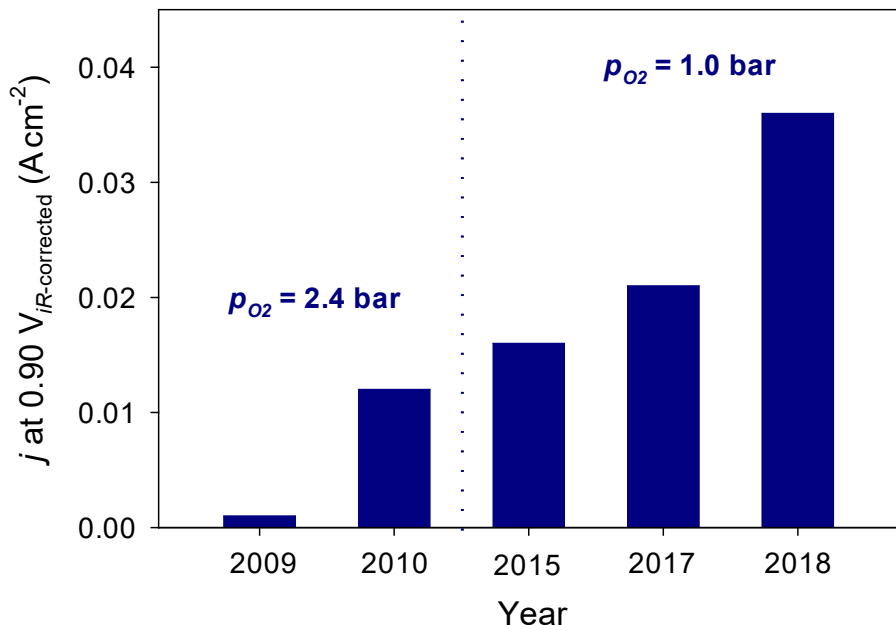


Degradation of (CM+PANI)-Fe-C(Zn): Operando XAFS



- FeN_x site undergoing oxidation during catalyst incorporation into MEA and during 0.7 V hold in oxygen
- Oxidation of Fe coincident with loss in performance
- Fe reduced back to original state during cathode purge with helium, but without a recovery in fuel cell performance
- Irreversible loss of active sites responsible for performance loss rather than structural or chemical alteration of remaining Fe-N/O centers

Progress in Fuel Cell Performance from 2008 to 2018

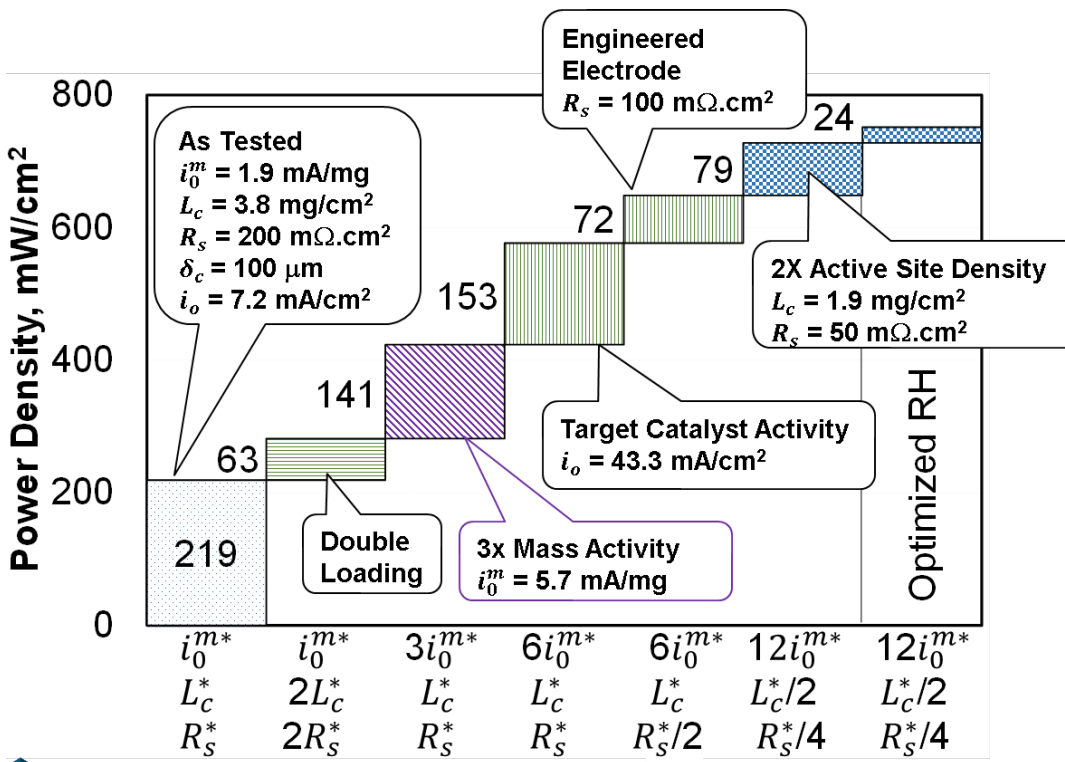


$\text{H}_2\text{-O}_2$ Voltage (iR -corrected)	j (Acm^{-2})				
	2009	2010	2015	2017	2018
0.90	0.001	0.012	0.016	0.021	0.036

Continuous improvement in fuel cell performance of PGM-free ORR catalysts maintained in the past decade ($\text{H}_2\text{-air}$ performance not recorded before 2013)

Paths Towards Power Density Improvement for PGM-free Cathodes

- Systematic improvements needed in catalyst activity and electrode structure to reach 1000 mW/cm² power density in a 90-kW_e stack while meeting Q/dT = 1.45 kW/°C target at 2.5 atm inlet pressure, 95 °C coolant exit temperature, and 1.5 cathode stoichiometry
- Advances needed:
 - ✓ Reduce kinetic losses by 12x mass activity increase
 - ✓ Reduce iR_{Ω}^c overpotential with 2x active site density and engineered electrode structure for 50% lower sheet resistance
 - ✓ Manage mass transfer losses with 0.5x electrode thickness



	(AD)Fe-N-C Catalyst	Advanced Catalyst
Mass Activity	1.9 mA/mg	22.6 mA/mg
Catalyst Loading	3.8 mg/cm ²	1.9 mg/cm ²
Catalyst Activity	7.2 mA/cm ²	43.3 mA/cm ²
Electrode Thickness	200 μm	50 μm
Sheet Resistance	200 mΩ.cm ²	50 mΩ.cm ²
Current Density	330 mA/cm ²	1150 mA/cm ²
Kinetic Loss	465 mV	405 mV
Ohmic Loss	40 mV	70 mV
Mass Transfer Loss	12 mV	35 mV

- Limited stability of PGM-free electrodes under steady-state and load-cycling conditions and under AST cycling, especially in air
- Still inadequate understanding of the catalyst and electrode degradation mechanism(s)
- PGM-free catalyst ORR activity in need of further improvement (12x current status required)
- Improved electrode design and catalyst-ionomer integration to provide adequate ionic, electronic, and mass transport to and from active sites
- Materials and synthetic techniques to increase active site density while avoiding spectator species formation (e.g., Fe metal clusters and carbides)
- Further development of radical scavenger into cathode layer to mitigate the effects of hydroperoxyl radical formation likely responsible for ionomer and/or carbon matrix degradation

- **ElectroCat Development**

- ✓ Downselect 2018 proposed national laboratory capabilities through Go/No-go decisions and utilize remaining capabilities to support core and FOA project efforts
- ✓ Incorporate collaborators from DE-FOA-0001874 into ElectroCat and coordinate activities of all ElectroCat partners
- ✓ Populate Data Hub with datasets from national laboratory and FOA partners; implement automated methods for data capture and publication
- ✓ Further develop automated supervised learning and machine learning techniques for data correlation and experimental design

- **Improvement in Performance and Durability of Catalysts and Electrodes**

- ✓ Further identify primary factors governing the durability of PGM-free catalysts and electrodes and continue to develop means to prevent performance degradation
- ✓ Advance fuel cell performance of catalysts by maximizing volumetric density and accessibility of active sites, through (i) the development of novel synthesis approaches, using information from *in situ* characterization techniques and (ii) optimization of hierarchical pore-size and ionomer distribution, using information from imaging, X-ray scattering, and multi-scale modeling efforts
- ✓ Determine and optimize fuel cell performance of highest activity high-throughput-synthesized materials; further explore synthetic conditions, dopants, and non-Fe metals
- ✓ Correlate probe desorption temperatures with site identity and poisoning of ORR activity

Any proposed future work is subject to change based on funding levels

- **ElectroCat Development and Communication**

- ✓ Consortium is supporting four existing and six new FOA projects with 10 capabilities
- ✓ A consortium-wide meeting was held on January 30-31, 2019 to kick off new FOA projects. Information distributed to consortium members; select information available through public website and data management hub (electrocatalysis.org; <https://datahub.electrocatalysis.org>)
- ✓ 12 papers published, 20 presentations given (10 invited)

- **Progress in Performance and Performance Durability**

- ✓ ElectroCat FY18 Annual Milestone of PGM-free cathode MEA performance of 25 mA cm^{-2} at $0.90 \text{ V (H}_2/\text{O}_2, iR\text{-free)}$ exceeded – high of 36 mA cm^{-2} , average of 33 mA cm^{-2} achieved
- ✓ Developed an (Fe,Zn)-ZIF catalyst precursor with Fe exclusively in FeN_4 sites, which, after heat treatment, resulted in a catalyst with no detectable Fe spectator species
- ✓ Addressed “shelf-life” durability of the (AD)Fe-N-C catalyst powder
- ✓ Dramatically improved performance stability and decreased CO_2 emissions of (CM+PANI)-Fe-C(Zn) cathodes under steady-state holds in O_2 using a radical scavenger

- **Characterization and Capability Development**

- ✓ Determined that performance loss of (AD)Fe-N-C cathode with AST cycling is predominantly due to loss of catalyst activity
- ✓ Determined using NRVS and Mössbauer spectroscopy that NO, the surface molecular probe, can bind to Fe^{3+} and Fe^{2+} ; quantified the amount of NO adsorbed at high and low potentials using voltammetric stripping and temperature-programmed desorption

- ✓ Used STEM-EELS and X-ray absorption to characterize Fe species and structure evolution during heat treatment, obtaining guidance for improved catalyst synthesis
- ✓ Characterized ORR activity and atomic structure of 75 high-throughput-synthesized Fe-dopant-phenanthroline-ZIF catalysts using X-ray absorption and multi-channel flow double electrode cell, identifying materials with $E_{1/2} > 0.8$ V
- ✓ Developed and utilized methods to characterize Fe speciation as a function of cell potential using *in situ* Mössbauer spectroscopy
- ✓ Acquired MEA performance and kinetic data for (AD)Fe-N-C cathode as a function of the number of AST cycles and applied the distributed ORR model to determine the kinetic losses, number of active sites remaining, and the mass transport losses
- ✓ Defined advances needed in catalyst activity and electrode properties to achieve 1000 mW/cm² power density while meeting Q/dT target

- **ORR active-site modeling**
 - ✓ Calculated DFT database of vibrational spectra with and without probe molecules for identification of stretching frequencies observed using nuclear resonance vibrational spectroscopy
 - ✓ Calculated DFT database of isomer shift and quadrupole splitting values for identification of doublets in Mössbauer spectra of PGM-free catalysts
- **Project performance measures**
 - ✓ ElectroCat milestones and quarterly progress measures (QPMs) for all four labs either completed or on track

Reviewers' Comments from 2018 Annual Merit Review (Continued)

- *“It is recommended that the project increase efforts on modeling the electrode structure and aligning a “possible” future catalyst design with an optimized model design. For example, it is suggested that the project take into account the realistic concentration of achievable active sites, electrode thickness, and transport effects. Efforts should be increased to understand the degradation mechanisms.”*

This effort has been increased this year. Please see slides 28 and 36 for a summary of the findings.

- *“Overall, the proposed future work is good, continuing fundamental studies across the breadth of topics necessary to advance the PGM-free activity class. Additional near-term work should assess carbon corrosion stability, one of the primary (and perhaps fundamental) barriers with carbon-based non-PGM catalysts.”*

FY19 work has addressed comments on carbon corrosion stability, as well as electrode structure optimization. Continuing durability studies will encompass further understanding of more graphitic carbon structures, e.g., MOF-based catalysts. Modeling and experimental studies are being carried out to further optimize the PGM-free electrode structures including use of carbon structures with increased active site density, as well as favored mass transport properties.

- *“Since this project introduces Fe into the catalyst, it must define a [peroxide] solution path.”*
“Carbon corrosion stability may be a likely key fundamental barrier, which should be assessed in the nearer term.”

While there is concern over carbon stability and hydroperoxyl radical generation, the highly graphitized PGM-free catalysts show low CO₂ emissions and decreased FER using radical scavengers.

- “Extensive *ex situ* and *in situ* characterization of PGM-free catalysts was done. However, the focus is primarily on **Fe-N-C**, and therefore, the ultimate usefulness of this work will be limited. **The high-throughput addresses only a narrow range of parameters that are expected to give only incremental improvements. Stability is not a criterion in high-throughput screening; it is hard to see any innovative approach that will significantly improve the volumetric activity and stability.**”

The parameter space has been widened this year, including alternative transition metals and addition of dopants intended to address the presumed peroxide-induced degradation.

- “*A method for estimating the demonstrated active site density will help with understanding and improving the active site structure. NO_2^- was successfully used as a molecular probe, but the catalyst will also have a nitrogen species, so it is uncertain if this is a Fe-N species interaction with a probe molecule.*”

Formation of NO on the catalyst surface has been confirmed by TPD, which also reveals very similar ratio between NO adsorbed at low and high potentials as determined from the stripping charges last year. DFT calculations show plausibility of reaction pathway during stripping (necessary for accurate density assignment). Finally, the data presented last year shows that upon exposure to nitrite a new Fe-N scattering path appears in the EXAFS data while the existing Fe-N paths are retained.



PGM-free catalyst development, electrochemical and fuel cell testing, atomic-scale modeling

Piotr Zelenay (PI), Hoon Chung, Siddharth Komini Babu, Ted Holby, Vijay Bhooshan Kumar, Ulises Martinez, Gerie Purdy, Turab Lookman, Xi Yin



High-throughput techniques, mesoscale models, X-ray studies, aqueous stability studies

Debbie Myers (PI), Jaehyung Park, Nancy Kariuki, Magali Ferrandon, Ted Krause, Ce Yang, Evan Wegener, A. Jeremy Kropf, Rajesh Ahluwalia, Xiaohua Wang, C. Firat Cetinbas, Voja Stamenkovic, Eric Coleman, Pietro Papa Lopes, Ian Foster, Ben Blaiszik, Marcus Schwarting

Advanced fuel cell characterization, rheology and ink characterization, segmented cell studies

K.C. Neyerlin (PI), Luigi Osmieri, Sadia Kabir, Scott Mauger, Guido Bender, Michael Ulsh, Sunil Khandavalli, Kristin Munch, Robert White, John Perkins

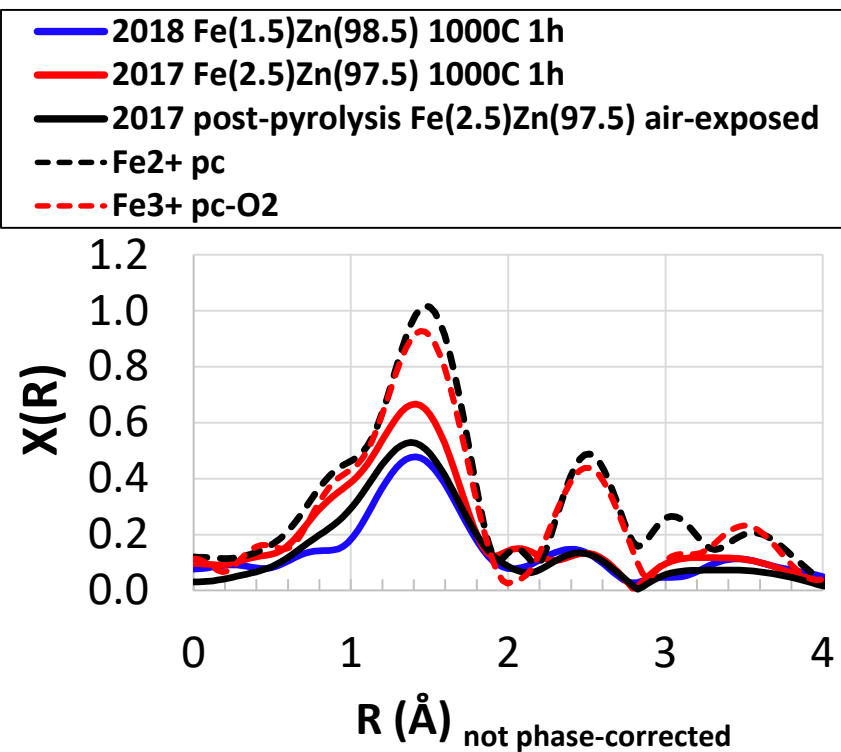
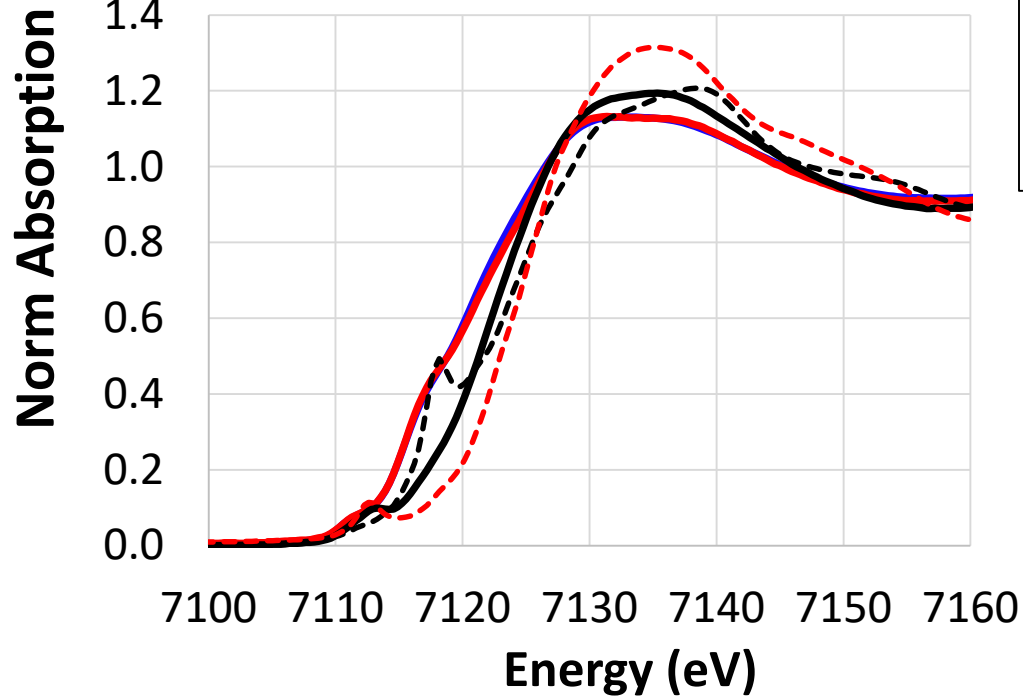
Advanced electron microscopy, atomic-level characterization, XPS studies

Karren More (PI), David Cullen, Harry Meyer III, Shawn Reeves

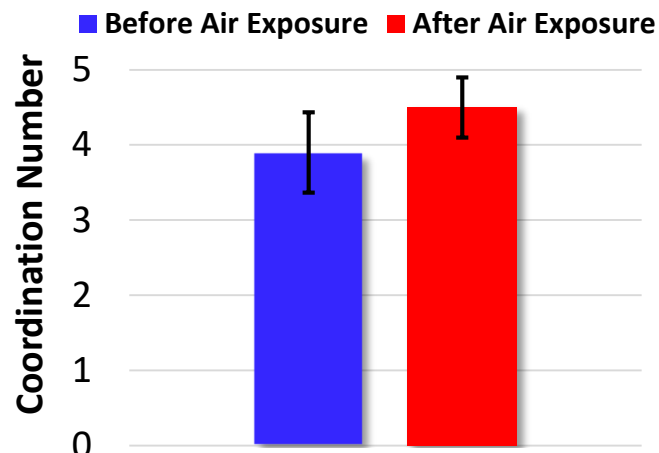


Technical Back-Up Slides

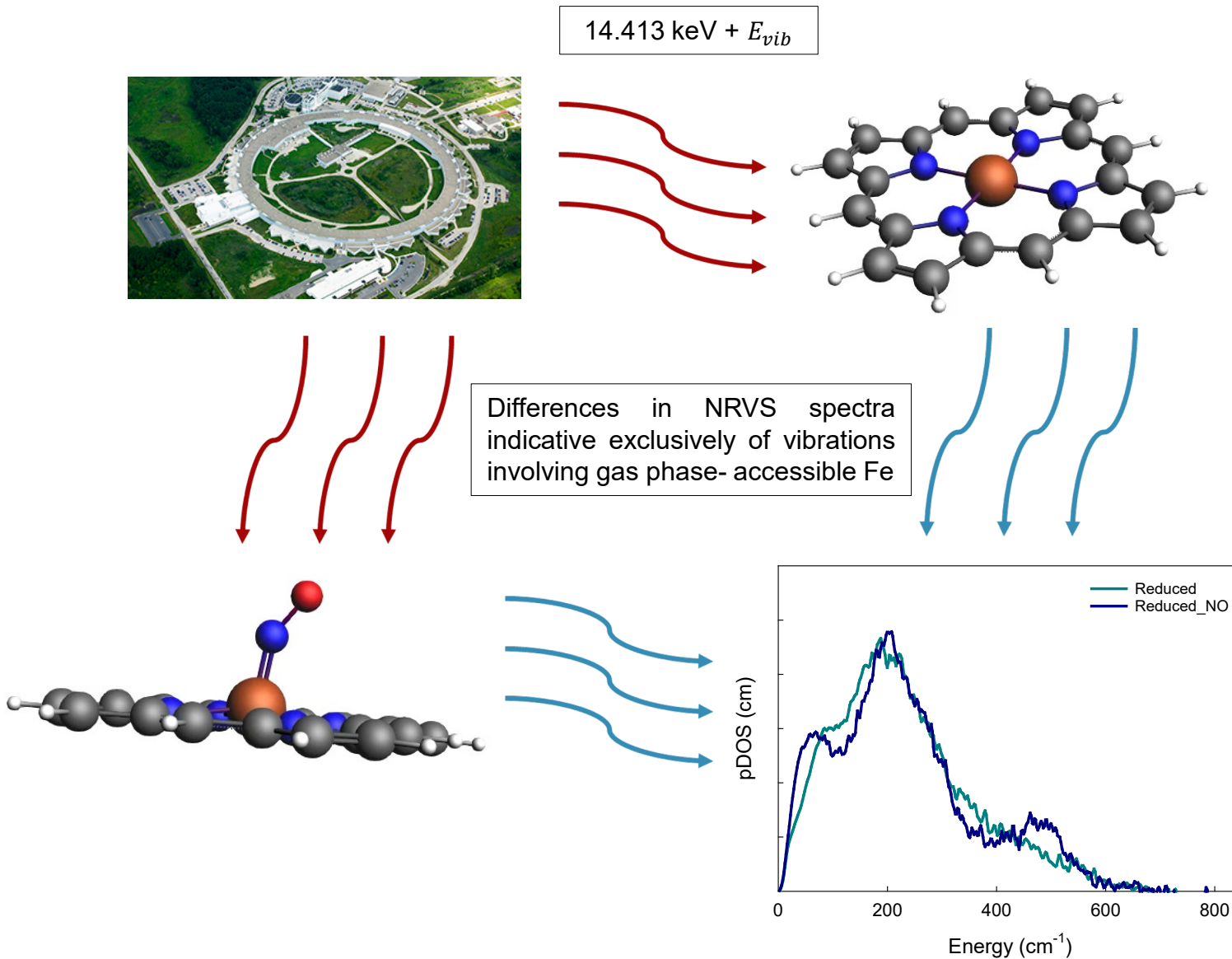
Comparison of $\text{Fe}_{2.5}$ and $\text{Fe}_{1.5}$ Zn ZIF XAFS During Pyrolysis



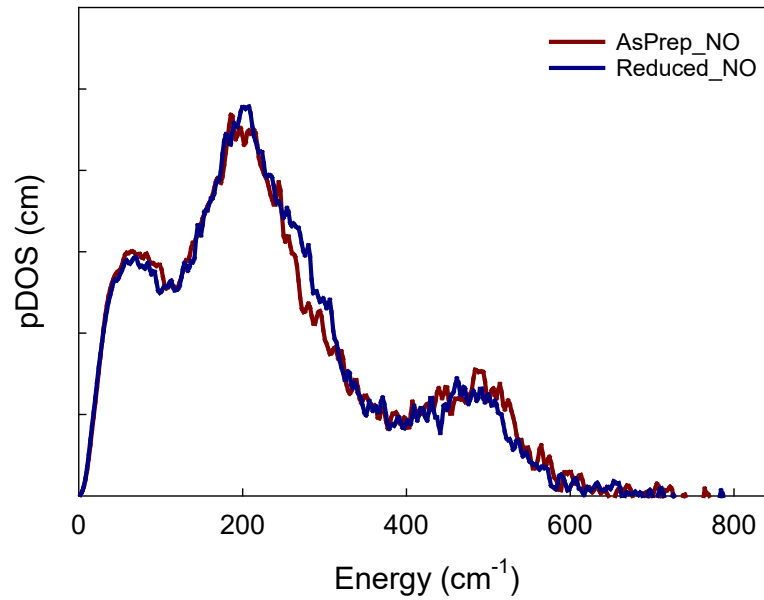
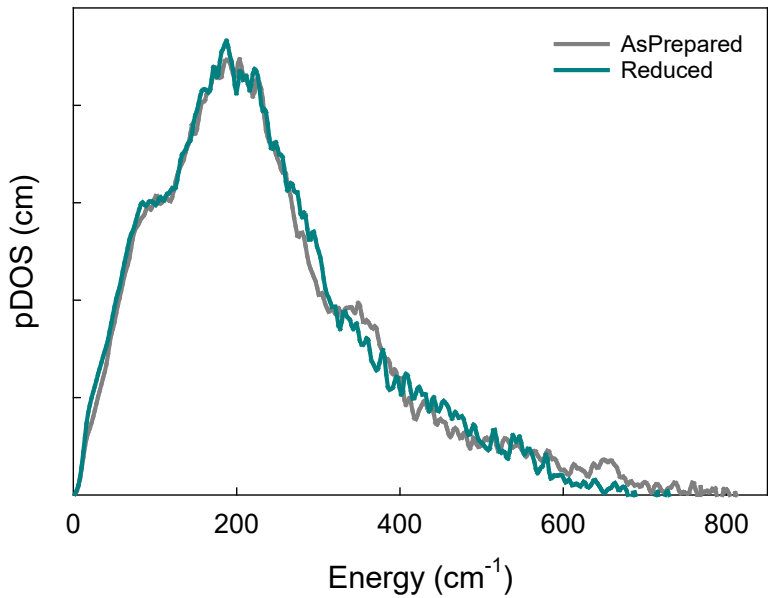
- After heat treatment at 1000°C, before exposure to air, $\text{Fe}_{2.5}\text{Zn}_{97.5}\text{-N-C}$ and $\text{Fe}_{1.5}\text{Zn}_{98.5}\text{-N-C}$ have nearly identical Fe coordination and oxidation state
 - ✓ Evidence of Fe^{2+} square pyramidal/octahedral and Fe^{2+} square planar coordination in XANES pre-peak
- Air exposure after heat treatment oxidizes majority of Fe^{2+} to Fe^{3+} , concomitant with increase in first shell coordination and appearance of a new scattering path



Nuclear Resonance Vibrational Spectroscopy (NRVS)

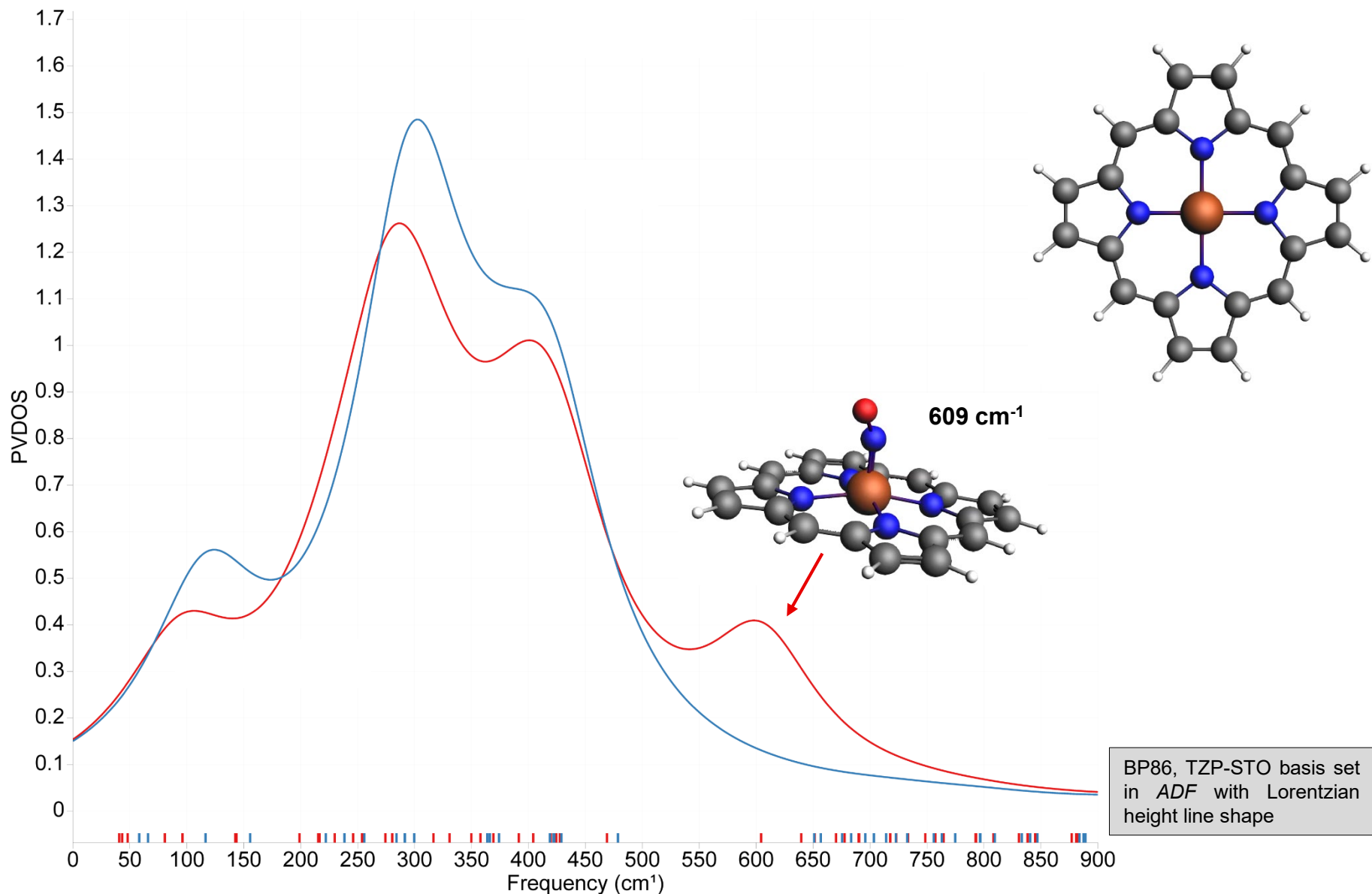


(AD)⁵⁷Fe-N-C Catalyst: NRVS with NO Probe Molecule

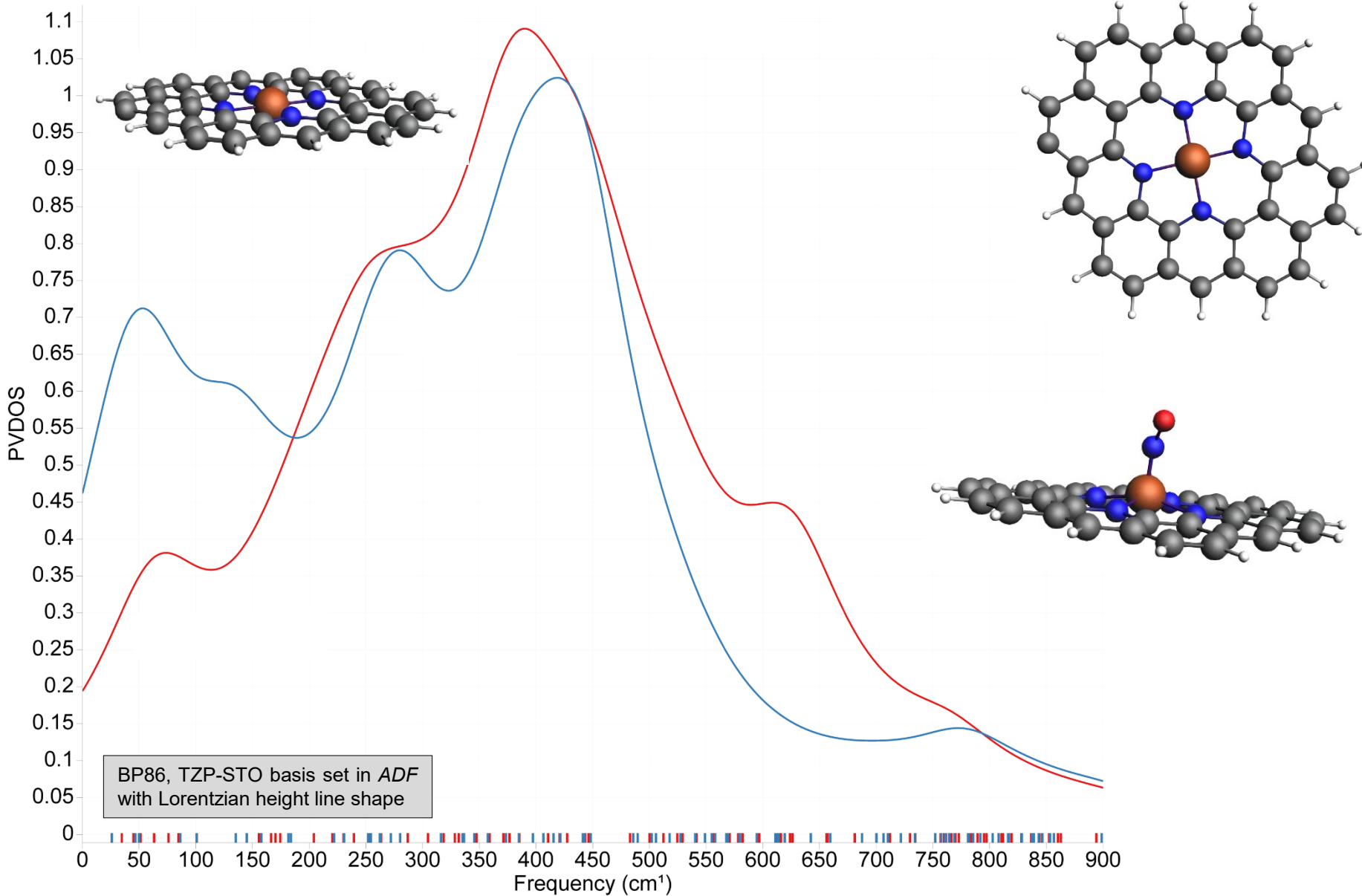


Nuclear resonance vibrational spectroscopy (NRVS) used with NO as a molecular probe (an O₂ analog) to detect iron sites on (AD)⁵⁷Fe-N-C catalyst; NO probe works for both Fe³⁺ and Fe²⁺

DFT Calculation: NRVS with NO Probe Molecule



DFT Calculation: NRVS with NO Probe Molecule



Goal: Calculate isomer shift and quadrupole splitting for hypothetical active-site structures for the main purpose of comparison with experimental values (*ex situ*, *in situ*, and with probe molecules); obtain Fe-specific signatures (Amsterdam Density Functional Suite, ADF)

Isomer Shift (δ) from calculated electron density at nucleus ($\rho(0)$):

$$\delta = \alpha(\rho(0) - c) + \beta$$

α , β , and c parameters from fit to 66 experimentally determined values for well characterized Fe structures

Quadrupole Splitting (E_Q) from calculated electric field gradient tensor (V) and quadrupole moment tensor at nucleus (Q)

$$E_Q = -\frac{e}{6} \sum_{a=1}^3 V_{aa} Q_{aa}$$

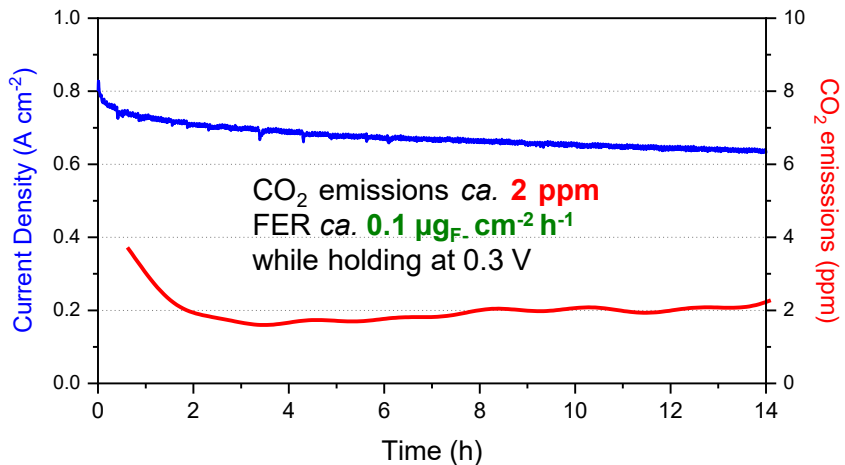
"On Predicting Mössbauer Parameters of Iron-Containing Molecules with Density-Functional Theory", Pápai and Vankó, *JCTC*, **9**(11), 2013, pp. 5004-5020.

Isomer Shift	– <i>mean average error 0.05 mm/s; maximum deviation 0.17 mm/s</i>
Quadrupole Splitting	– <i>mean average error 0.25 mm/s; maximum deviation 1.29 mm/s</i>

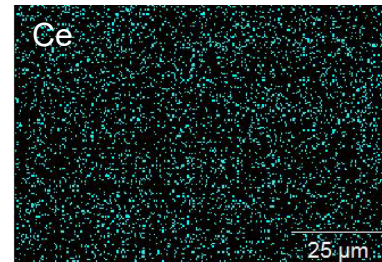
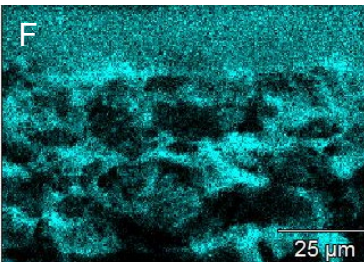
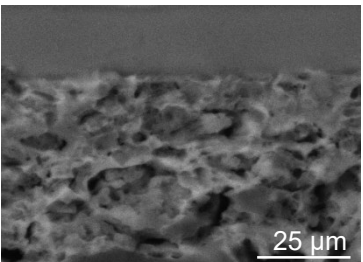
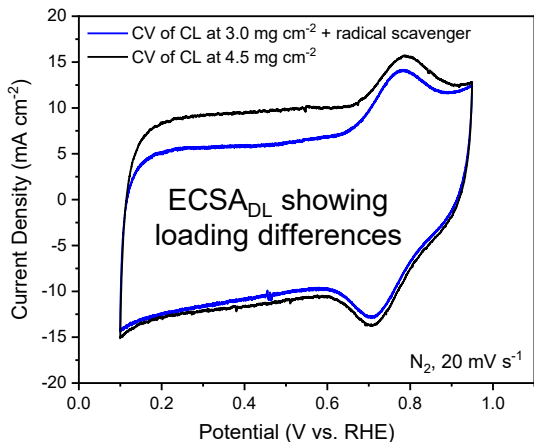
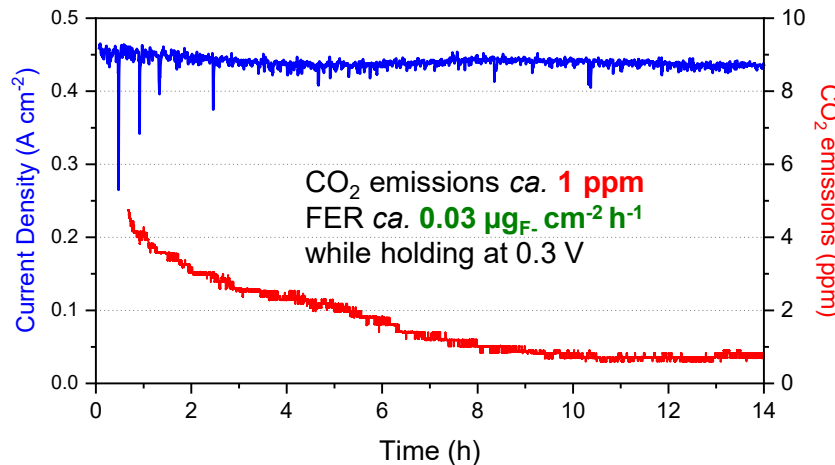
(CM+PANI)-Fe-C(Zn) Catalyst Durability with and without Radical Scavenger

Anode: 0.2 mg_{Pt} cm⁻² Pt/C H₂, 200 sccm, no backpressure; Cathode: ca. 4.5 mg cm⁻² (CM+PANI)-Fe-C(Zn) or ca. 3.0 mg cm⁻² (CM+PANI)-Fe-C(Zn) + 5 wt.% radical scavenger, air, 500 sccm, no backpressure; Cell: Nafion[®]211; 5 cm²; 80 °C; 100% RH, constant voltage: 0.3 V

(CM+PANI)-Fe-C(Zn) without radical scavenger



(CM+PANI)-Fe-C(Zn) + 5 wt.% radical scavenger

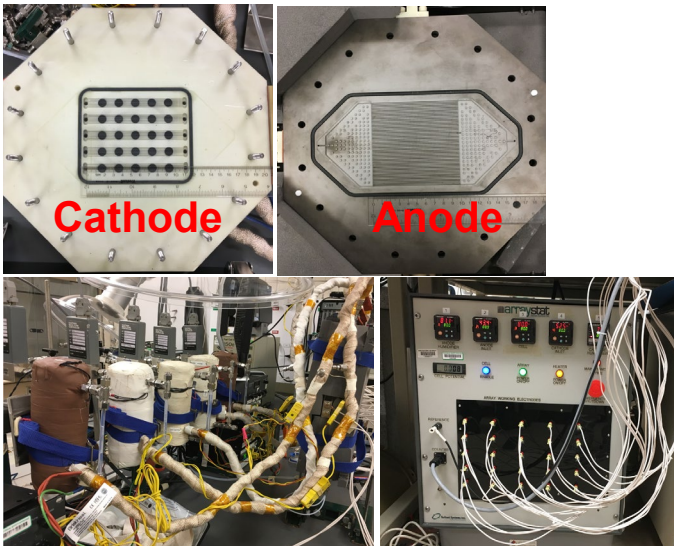


After testing no large radical scavenger particles found,
Ce distributed throughout the catalyst layer

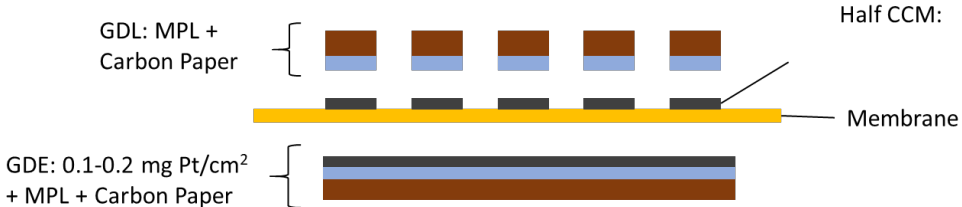
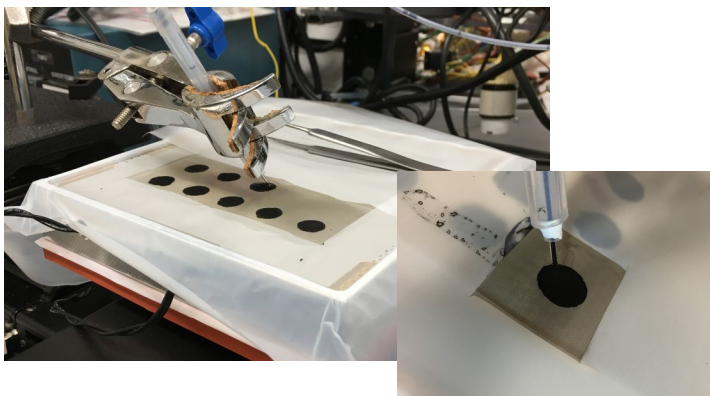
Combinatorial Fuel Cell Performance Testing

NuVant 25 Segmented Electrode Hardware:

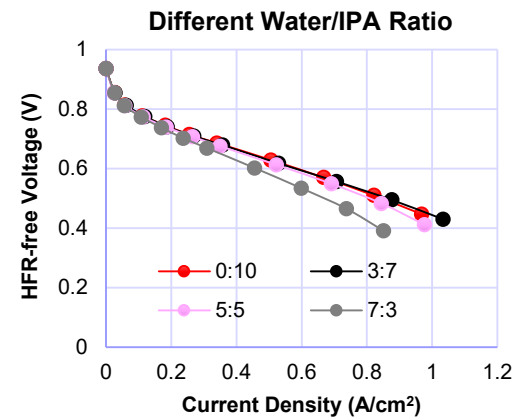
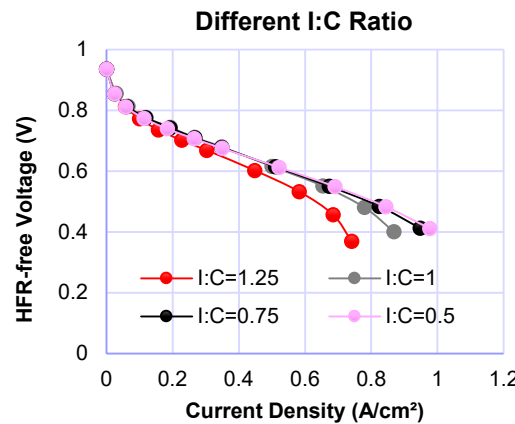
- High-throughput MEA test set up to expedite PGM-free electrode performance testing.



Developed system for automated ink deposition onto heated membrane to make 25-electrode catalyst-coated membrane



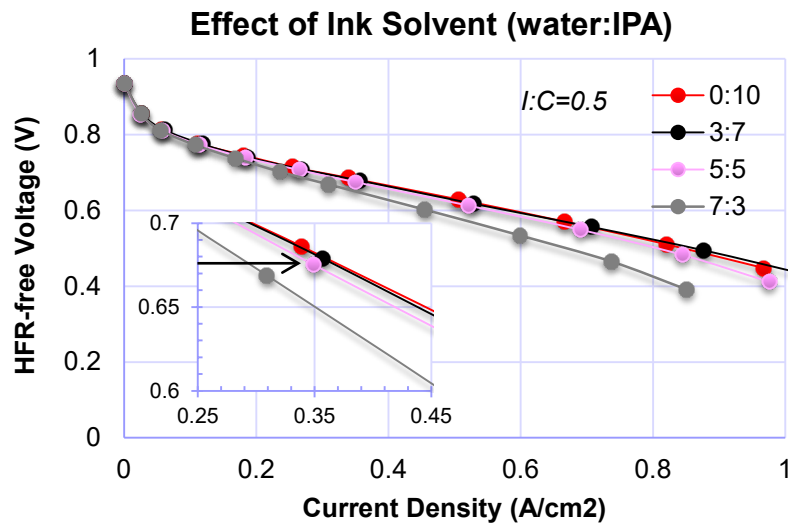
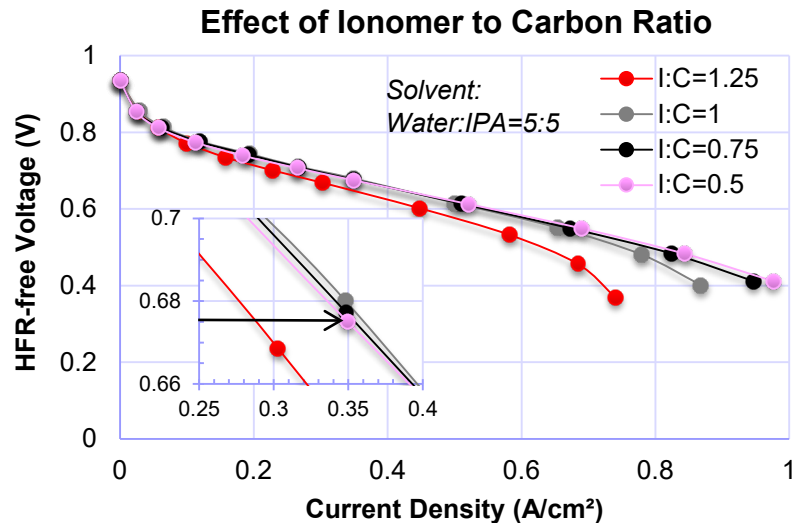
Effect of I:C ratio and solvent on Performance



Anode: $0.2 \text{ mg}_{\text{Pt}}/\text{cm}^2$ onto 29BC GDL
Cathode: half CCM, Atomically-dispersed Fe catalyst, University of Buffalo 2.5 at% Fe MOF-derived catalyst from Carnegie Mellon University-led project, $4 \text{ mg}_{\text{cat}}/\text{cm}^2$
Cell temperature: 80°C ; Flow rate H_2/air : 200/200 sccm, RH: 100%, 1 bar H_2/air partial pressure; Nafion XL

Combinatorial Fuel Cell Performance Testing

- High-throughput MEA test set up to expedite PGM-free electrode performance testing
- Automated ink deposition onto heated membrane to make 25-electrode catalyst-coated membrane
- University at Buffalo ZIF-derived catalyst performance optimization using the high-throughput / combinatorial MEA test set up



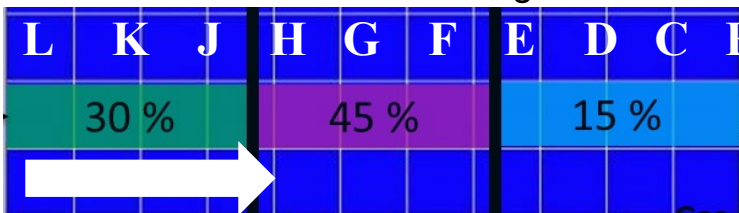
Anode: 0.2 mg_{Pt}/cm² onto 29BC GDL

Cathode: half CCM, Atomically-dispersed Fe catalyst, University of Buffalo 2.5 at% Fe MOF-derived catalyst from Carnegie Mellon University-led project, 4mg/cm². Cell temperature: 80°C; Flow rate H₂/air: 200/200 sccm, RH: 100%, 1 bar H₂/air partial pressure; Nafion XL

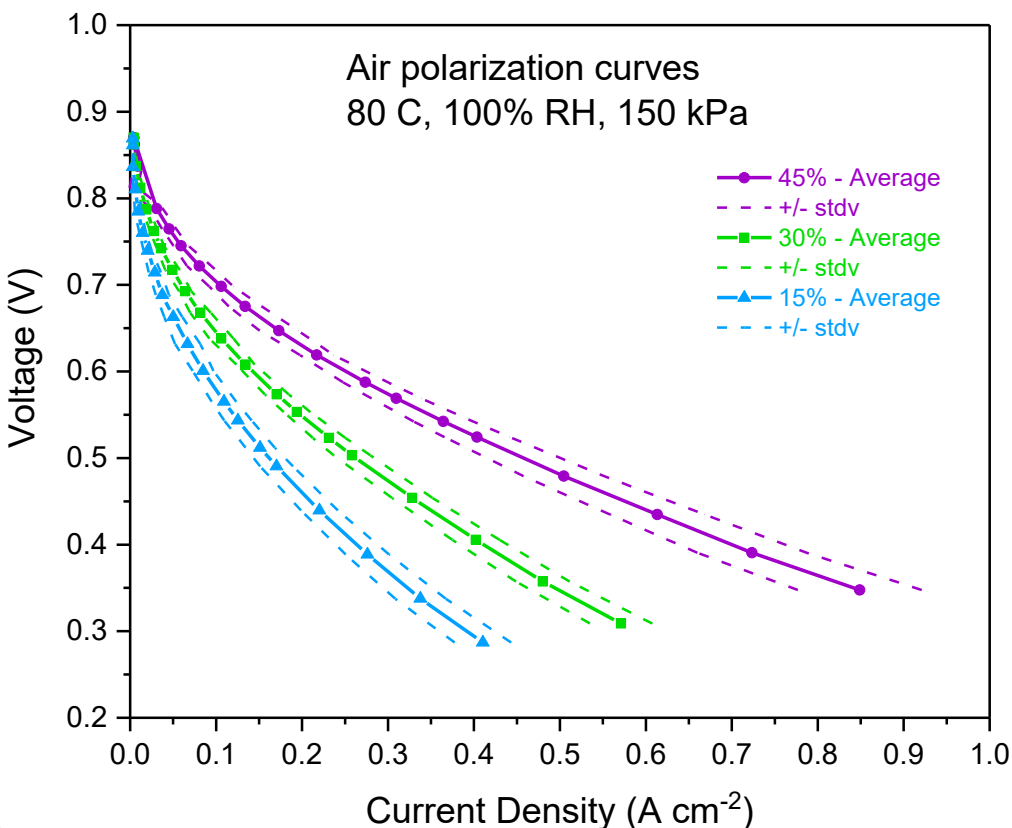
- I/C of 0.5 gives the highest hydrogen-air cell performance at < 0.65 V while an I/C of 1 gives the highest performance at > 0.65 V.
- The power density at 0.675 V was increased by 3% using an I/C of 1 versus the baseline I/C of 0.5.
- IPA to water ratio of 3:7 shows the highest overall performance.
- At 0.675 V, the electrodes fabricated from the pure IPA solvent showed a slightly better performance than those fabricated from the 3:7 solvent, with an increase of 6% in power density that obtained with the electrode made from the 5:5 solvent composition baseline.

Differential Combinatorial Cell for Optimizing Electrode Composition

One of several tested configurations:



Pajarito Powder Catalyst:
15, 30, and 45% Ionomer Content



- Differential operation of cell
- Combinatorial sample using electrode with three different ionomer loadings
- Capability to discern differences in performance
- Results confirmed to be independent from:
 - ✓ Flow direction
 - ✓ Location in cell

⇒ Rapid prototyping of various combinations in single experiment

